Project no. ICT-257159

Project acronym:

MACALO

PROJECT TITLE: MAGNETO CALORITRONICS

Area: Nanoelectronics Technology (ICT-2009.3.1)

1st Intermediate report

Deliverable EVAL-1

Due date of deliverable: M12
Actual submission date: 1/9/2011

Start date of project: 01/09/2010 Duration: 36 Months

Organization name of lead contractor for this deliverable: UT

Del. no.	Deliverable name	WP no.	Nature	Dissemination level[1]	Delivery date (proj month)
D5.1	EVAL-1	5	RTD	PU	12

[1] **PU** = Public
PP = Restricted to other programme participants (including the Commission Services).
RE = Restricted to a group specified by the consortium (including the Commission Services).
CO = Confidential, only for members of the consortium (including the Commission Services).
Make sure that you are using the correct following label when your project has classified deliverables.
EU restricted = Classified with the mention of the classification level restricted "EU Restricted"
EU confidential = Classified with the mention of the classification level confidential " EU Confidential "
EU secret = Classified with the mention of the classification level secret "EU Secret "

First-principles calculations of the Gilbert damping, resistivity and spin diffusion length for magnetic multilayers with perpendicular anisotropy

Yi Liu, Zhe Yuan, Anton A. Starikov, and Paul J. Kelly
Faculty of Science and Technology and MESA$^+$ Institute for Nanotechnology, University of Twente, P.O. Box 217, 7500 AE Enschede, The Netherlands
(Dated: September 19, 2011)

We perform a systematic study of the spin-flip diffusion length, resistivity and Gilbert damping parameter in Co|X magnetic multilayers where X=Cu, Ni, Pd and Pt. The first-principles calculations are carried out within the framework of scattering theory and temperature is accounted for by means of a frozen thermal lattice disorder scheme. Our results should provide useful guidance in choosing suitable materials for experimental spintronics investigations.

PACS numbers: 72.25.Ba, 72.25.Rb, 72.10.Di

I. INTRODUCTION

The discovery in layered magnetic structures[1] of oscillatory exchange coupling, giant magnetoresistance (GMR), perpendicular magnetic anisotropy (PMA), large magnetooptical effects, spin-current induced magnetization excitation and reversal has revealed a wealth of new phenomena that open up numerous possibilities for applications. The spin-transfer torque (STT) predicted by Slonczewski[2] and Berger[3] and subsequently confirmed by experiment[4–11] forms the basis for new forms of data storage, so-called Magnetic Random Access Memories (MRAM),[12,13] where magnetic bits are read and written using the GMR and STT effects or for tunable microwave sources, so-called spin-torque oscillators (STO).[14] In the endeavour to reduce the currents required to operate these devices, an important step has been the introduction of materials with large PMA such as Co|Pt and Co|Ni multilayers.[15–18] The device performance is determined by fundamental transport properties of these multilayers (ML), such as the spin-flip diffusion length and Gilbert damping frequency that restrict the operating length- and time-scales. However, current experimental measurements with a variety of ML structures yield a wide spread of parameter values.[19–21] A better understanding of which factors contribute to the numerical values of these fundamental parameters would be useful in choosing materials appropriate to specific applications.

It is the purpose of this paper to provide a first study of the resistivity, Gilbert damping and spin-flip diffusion in magnetic multilayers exhibiting PMA using a muffin-tin orbital (MTO) based scattering formalism that includes spin-orbit coupling and disorder that was recently applied to a study of these properties in ferromagnetic alloys[22] and crystalline Fe, Co and Ni.[23] A MTO-based electronic structure scheme was earlier used to study the occurrence of PMA in multilayers comprising the $3d$ itinerant ferromagnetic materials Fe and Co and late $4d$ or $5d$ non-magnetic metals[24] where it proved to have predictive capability.[25,26] A key issue in the present study will be to determine whether and how properties that are strongly dependent on the spin-orbit coupling are correlated in the Co|X multilayers (X=Ni, Pd, and Pt) that are extensively studied and applied in spin-transfer devices.[16,19,27,28]

The dynamics of a magnetization $\mathbf{M}$ in an effective field $\mathbf{H}_{\rm eff}$ is usually described using the phenomenological Landau-Lifshitz-Gilbert equation

$$\frac{d\mathbf{M}}{dt} = -\gamma\mathbf{M}\times\mathbf{H}_{\rm eff} + \mathbf{M}\times\left[\frac{\lambda(\mathbf{M})}{\gamma M_s^2}\frac{d\mathbf{M}}{dt}\right], \qquad (1)$$

where $M_s = |\mathbf{M}|$ is the saturation magnetization and $\gamma = g\mu_B/\hbar$ the gyromagnetic ratio expressed in terms of the Landé g factor and the Bohr magneton μ_B. The first term describes the precessional motion of the magnetization in the effective field that includes the external applied field, the exchange field, anisotropy and demagnetization fields. The second term describes the time decay of the magnetization precession, the Gilbert damping,[29] in terms of $\lambda(\mathbf{M})$ that is in general a symmetric 3×3 tensor.[30] For isotropic media, the damping is frequently expressed in terms of the dimensionless parameter α given by the diagonal element of λ, $\alpha = \lambda/\gamma M_s$.

If a nonequilibrium magnetization is generated in a disordered ferromagnet (for example, by injecting a current through an interface), its spatial decay is described by the diffusion equation

$$\frac{\partial^2\Delta\mu}{\partial z^2} = \frac{\Delta\mu}{l_{\rm sf}^2}, \qquad (2)$$

where $\Delta\mu$ is the difference between the spin-dependent electrochemical potentials μ^σ for up and down spins, and $l_{\rm sf}$ is the spin-flip diffusion length.[31,32]

In this paper we calculate the spin-flip diffusion length $l_{\rm sf}$, resistivity ρ, and Gilbert damping parameter α for a series of MLs with PMA: $Co_1|Ni_{2(5)}$, $Co_1|Pd_2$, and $Co_1|Pt_2$, as well as $Co_1|Cu_2$ with an in-plane magnetization for comparison. To do so, we combine the scattering theory formulation of Gilbert damping[33] with frozen thermal lattice disorder[23] to model finite temperature lattice effects which are relevant since most measurements are carried out at room temperature. The calculated results can be understood based upon interface structure and spin-orbit coupling (SOC).

The paper is organized as follows. In Sec. II, a brief description of the scattering theory is given followed by some technical details of how the calculations are performed and how the spin-flip diffusion length, the resistivity and Gilbert damping parameter are determined. The results are presented and discussed in Sec. III. A short summary and some concluding remarks can be found in Sec. IV.

II. THEORETICAL METHODS AND COMPUTATIONAL DETAILS

The formulation of magnetization damping in terms of scattering theory has been shown to be equivalent in the linear response regime to the Kubo formalism.[33] In the scattering formalism, the Gilbert damping tensor $\tilde{G}$ can be expressed as

$$\tilde{G}_{i,j}(\mathbf{m}) = \lambda \cdot V = \frac{\gamma^2 \hbar}{4\pi} \mathrm{Re} \left\{ \mathrm{Tr} \left[\frac{\partial S}{\partial m_i} \frac{\partial S^\dagger}{\partial m_j} \right] \right\} \quad (3)$$

for a single domain ferromagnetic metal (FM) sandwiched between left- and right-hand leads of nonmagnetic (NM) material. The scattering matrix $S = \begin{pmatrix} r & t' \\ t & r' \end{pmatrix}$ is composed of reflection and transmission matrices for Bloch waves incident from the left (r and t) or right (r' and t') leads. When SOC is included, S depends on the direction of the magnetization unit vector $\mathbf{m} = \mathbf{M}/M_s$. The microscopic picture of magnetization damping implicit in the scattering formulation is that energy is transferred from the spin degrees of freedom through disorder scattering and SOC to the electronic orbital degrees of freedom that is rapidly lost to phonon degrees of freedom in thermal reservoirs attached to the leads. From the transmission matrices we can also calculate the conductance of the system within the Landauer-Büttiker formulation as $G = (e^2/h)\mathrm{Tr}\left\{tt^\dagger\right\}$. In collinear ferromagnetic systems, we can project every propagating state onto the global quantization axis and determine the spin-resolved conductance $G^{\sigma\sigma'}$ with $\sigma = \uparrow, \downarrow$.

To calculate the scattering matrix at the Fermi level, we use a "wave-function matching" scheme[34] implemented with tight-binding linearized muffin-tin orbitals (TB-LMTOs)[35,36] that was recently extended to include SOC.[22] The electronic structure of the NM|FM|NM sandwich is first determined self-consistently using a surface Greens function method[37] with a minimal basis of TB-LMTOs in the atomic sphere approximation. In the current study of (111) oriented $\mathrm{Co_1|X}_n$ MLs with n=2 for X=Cu, Pd, Pt, and n=2,5 for X=Ni, we consider a ML consisting of close-packed Co and X planes stacked in an $ABCABC\ldots$ sequence that is attached to matching (111) oriented fcc Cu leads. This corresponds to a current-perpendicular-to-the-plane (CPP) geometry. Since the experimental lattice constants for the constituent bulk materials are quite similar, we calculate the lattice constants for the $\mathrm{Co_1|Cu_2}$ and $\mathrm{Co_1|Ni_{2(5)}}$ ML structures using Vegard's law forcing the Cu leads to match in plane.[38] For $\mathrm{Co_1|Pd_2}$ and $\mathrm{Co_1|Pt_2}$, we fix the (111) in-plane lattice constants to be the values calculated for bulk fcc Pd and Pt, and then determine layer distances[24] by total energy minimization using the Vienna ab-initio simulation package (VASP)[39–41] to calculate the density functional theory electronic energies. The in-plane lattice constants of the Cu leads are stretched to match the ML.[42] We will demonstrate that the properties we are interested in are independent of how the leads are modelled.

Without disorder, it is not possible to calculate resistivity, Gilbert damping or spin-flip scattering for defect-free multilayers. We introduce thermal disorder in the scattering region in the form of "frozen thermal lattice disorder" by displacing atomic spheres rigidly and randomly from their ideal lattice positions in large lateral supercells[23] and characterize it by the root-mean-square (rms) displacement Δ. To determine values of Δ in the various ML systems, we have first carried out *ab initio* phonon calculations[43] for bulk fcc Cu, Ni, Pd, and Pt. We then populate the phonon modes with a Boltzmann distribution at a certain temperature to obtain the relative rms displacement Δ/a_0, where a_0 is the corresponding fcc lattice constant. In the scattering region consisting of a Co|X magnetic ML, the atomic displacements on Co atoms are scaled by the factor of $\sqrt{m_\mathrm{X}/m_\mathrm{Co}}$, where m are the atomic masses. Throughout the paper, all temperatures were simulated in this way.

For the magnetic ML of thickness L, we calculate the spin-resolved components of conductance $G^{\sigma\sigma'}(L)$. The spin conductance is $G^\sigma = \sum_{\sigma'} G^{\sigma\sigma'}$ and the total conductance is $G(L) = \sum_\sigma G^\sigma$. The bulk asymmetry parameter β is given by the asymptotic values of the fractional spin conductances G^σ/G and the spin-flip diffusion length l_sf can be determined by fitting G^σ/G as a function of L using Eq. (6) from Ref. 22, as shown in Fig. 1(a) for a $\mathrm{Co_1|Ni_2}$ multilayer with frozen thermal lattice disorder.

If we write the total resistance of the system as $R(L) = 1/G(L) = 1/G_\mathrm{Sh} + 2R_\mathrm{if} + R_\mathrm{b}(L)$, where G_Sh is the Sharvin conductance of the ideal leads, R_if is the NM|FM interface resistance and $R_\mathrm{b}(L) \approx \rho L$ is the bulk contribution,[34,44] we can determine the resistivity ρ from the slope of the total resistance as shown in Fig. 1(b). We can similarly write the total damping parameter as $\tilde{G}(L) = \tilde{G}_\mathrm{if} + \tilde{G}_\mathrm{b}$, where the interface contribution is $\tilde{G}_\mathrm{if}$ and the bulk contribution is $\tilde{G}_\mathrm{b}(L) = \lambda V = \alpha\gamma M_s A L$ with A the cross section. The dimensionless damping parameter α is then extracted from the slope of the total damping as shown in Fig. 1(c). Whereas l_sf, ρ, and α are all determined from the length dependence of the conductances and total damping, the leads only influence the intercepts of the curves in Fig. 1. This is the reason why the stretched Cu leads for $\mathrm{Co_1|Pd_2}$ and $\mathrm{Co_1|Pt_2}$ do not affect our results.

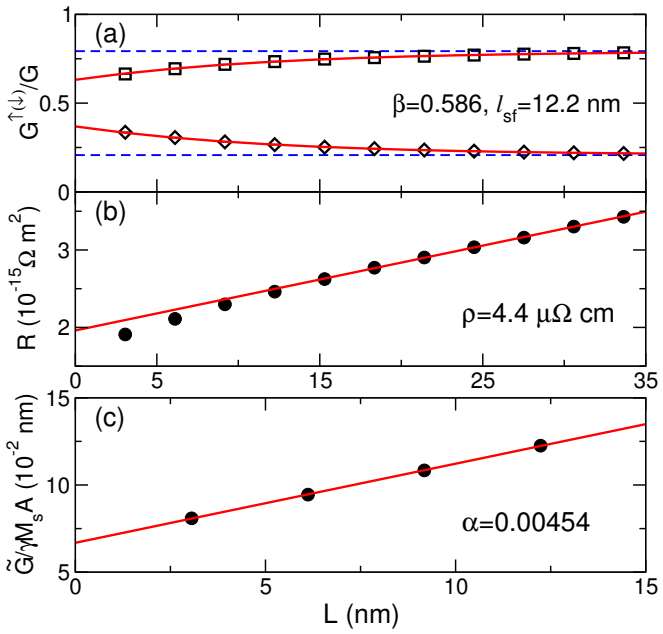

FIG. 1. (a) Fractional spin conductances for majority (squares) and minority (diamonds) spins, (b) total resistance and (c) total damping as a function of the thickness L of a $Co_1|Ni_2$ magnetic multilayer with frozen thermal lattice disorder. The root-mean-square atomic displacement Δ is determined by populating *ab initio* phonon modes of bulk fcc Ni at 300 K. The solid lines in each panel show the best fit to extract the spin-flip diffusion length l_{sf} (a), the resistivity ρ (b), and the Gilbert damping parameter α (c). The dashed horizontal lines in panel (a) denote the asymptotic values $(1 \pm \beta)/2$.

III. RESULTS AND DISCUSSION

We performed calculations for $Co_1|X_2$ (X=Ni, Cu, Pd, and Pt) and $Co_1|Ni_5$ MLs and the resulting resistivities are listed in Table I. For all systems, the resistivity increases monotonically with temperature. At each temperature, the resistivity of $Co_1|Ni_2$ is always lower than that of $Co_1|Cu_2$ although bulk Ni generally has a higher resistivity than bulk Cu. This can be understood in terms of the (111) interface resistance between Co and Ni being lower than that between Co and Cu because the similar Fermi surfaces of Co and Ni give rise to a larger transmission of propagating states at the Fermi level. This suggests that the resistivity of $Co_1|X_2$ is determined more by the interface resistance between Co and X than by the "bulk" resistivity of only two layers of X. Consistent with this is our finding that although Pd and Pt have nearly the same bulk resistivities, the resistivity of $Co_1|Pd_2$ is much lower than that of $Co_1|Pt_2$. When the Ni thickness is increased from $Co_1|Ni_2$ to $Co_1|Ni_5$, the resistivity of the ML rises slightly.

TABLE I. Calculated resistivities of magnetic MLs with CPP geometry.

ρ ($\mu\Omega$ cm)	200 K	300 K	400 K
$Co_1|Cu_2$	5.0±0.3	7.0±0.3	8.4±0.4
$Co_1|Ni_2$	3.9±0.2	4.4±0.2	5.3±0.3
$Co_1|Pd_2$	5.7±0.3	7.5±0.5	10.2±0.6
$Co_1|Pt_2$	21.5±0.7	28.2±0.9	35.4±0.9
$Co_1|Ni_5$	4.5±0.2	5.5±0.3	6.4±0.3

It has been found that l_{sf} is approximately proportional to $1/\rho$;[45] increasing disorder increases the resistivity and reduces the spin-flip diffusion length. This relation also holds qualitatively in our ML calculations as can be seen in Table II where the spin-flip diffusion lengths, l_{sf}, and bulk asymmetry parameters, β, calculated for the same magnetic MLs are listed. l_{sf} is seen to decrease with temperature for all MLs. A larger ρ in Table I corresponds to a smaller l_{sf} in Table II with the exception of Co|Ni.

At each temperature, $Co_1|Ni_2$ has a slightly shorter l_{sf} than $Co_1|Cu_2$ even though its resistivity is lower. This counterintuitive result can be understood in the following way. Though the strength of the SOC for Ni and Cu d electrons is very similar,[46] the spin-flip scattering of the d electrons at the Fermi level in Ni is stronger than that of the conduction s electrons in Cu. Increasing the Ni thickness going from $Co_1|Ni_2$ to $Co_1|Ni_5$, l_{sf} is found to increase a little because $Co_1|Ni_5$ is more like bulk Ni which has a longer l_{sf}. For the series $Co_1|Ni_2$, $Co_1|Pd_2$, and $Co_1|Pt_2$, the spin-diffusion length decreases significantly as the strength of the SOC increases.

Unlike the spin-diffusion length, the bulk spin asymmetry of the magnetic MLs is found to have a very weak temperature dependence. Its value reflects the ratio of the majority and minority spin resistivities. In $Co_1|X_2$ systems where the resistivities are largely determined by band mismatch at the Fermi level, the ratio is scarcely influenced by the thermal lattice disorder in the temperature range considered. β for Co|Ni is effectively reduced by increasing the thickness of Ni from $Co_1|Ni_2$ to $Co_1|Ni_5$ because β for bulk Ni is much smaller. The ML with the smallest value of β is $Co_1|Pt_2$ with $\beta \sim 0.2 - 0.25$, presumably because the spin-orbit coupling of Pt is much stronger than any that of any other element considered.

The calculated Gilbert damping parameters α are listed in Table III. Unlike ρ or l_{sf}, α does not exhibit a consistent temperature dependence for different MLs. For $Co_1|Ni_2$ and $Co_1|Ni_5$, α shows a very weak temperature dependence, while it increases for $Co_1|Pd_2$ and decreases for $Co_1|Pt_2$ from 200 K to 400 K. If the $Co_1|Cu_2$ magnetization is taken to lie in the plane of the ML, the damping is anisotropic when the magnetization is precessing parallel ($\alpha_\parallel$) and perpendicular ($\alpha_\perp$) to the plane. The average α value and the two anisotropic components all vary nonmonotonically with the temperature. All of this temperature dependence can be explained in terms of the following two observations:[23,47,48] (i) the Gilbert damping of bulk Co has a remarkably nonmonotonic dependence on the temperature, while (ii) the damping of bulk Ni, which is much larger than that of Co, decreases

TABLE II. Calculated spin-diffusion length l_{sf} and bulk asymmetry β of magnetic MLs with CPP geometry.

$l_{\rm sf}$ (nm), β	200 K		300 K		400 K	
$Co_1|Cu_2$	18.5±1.5	0.563±0.010	13.0±0.7	0.565±0.002	9.6±1.0	0.563±0.005
$Co_1|Ni_2$	13.4±1.0	0.558±0.010	12.2±0.5	0.586±0.003	9.0±0.2	0.579±0.003
$Co_1|Pd_2$	14.7±0.7	0.536±0.007	10.6±0.4	0.525±0.004	8.6±0.2	0.517±0.002
$Co_1|Pt_2$	6.2±0.6	0.242±0.003	5.1±0.5	0.228±0.001	3.9±0.8	0.206±0.002
$Co_1|Ni_5$	14.2±0.4	0.486±0.004	13.4±1.2	0.502±0.007	9.5±0.3	0.489±0.001

dramatically at low temperature with increasing temperature and begins to saturate around 200 K. If the damping is dominated by Ni in the Co|Ni systems, it would be expected to show little temperature dependence in the calculated temperature range. This scenario is supported by the finding that $Co_1|Ni_5$ has a larger α than $Co_1|Ni_2$ because it is more Ni-like. In the Co|X (X=Cu, Pd, Pt) systems, the damping behavior of Co is strongly influenced by X resulting in different temperature dependences. It has been suggested by Gilmore *et al.* that the Gilbert damping is proportional to the second or third power of the SOC strength,[49] thus α increases dramatically in the series $Co_1|Ni_2$, $Co_1|Pd_2$, and $Co_1|Pt_2$.

In real multilayers, a certain amount of interface mixing is unavoidable and the corresponding disorder will also give rise to electronic scattering and Gilbert damping. To examine the effect of interface mixing, we calculated ρ, $l_{\rm sf}$, and α for multilayers where we randomly exchanged a certain percentage of the atoms from adjacent layers. Taking $Co_1|Ni_2$ as an example, we prepare a series of $Co_{1-2x}Ni_{2x}|Ni_{2(1-x)}Co_{2x}$ with the interface mixing characterized by the concentration $2x$ of Ni atoms in the Co layer. As a function of $2x$, the spin-flip diffusion length $l_{\rm sf}$, resistivity ρ and Gilbert damping parameter α at zero temperature are plotted in Fig. 2 (solid black dots). The temperature dependent values listed in the tables are also included (empty red symbols) at zero mixing. As the mixing increases, $l_{\rm sf}$, ρ and α all tend to saturate around the corresponding values of the homogeneous alloy $Co_{33}Ni_{67}$ (dashed lines). At $2x$=16% where each Ni layer has 1 in 6 Ni atoms replaced by a Co atom, $l_{\rm sf}$ and ρ are not fully saturated, while α is. If we introduce thermal disorder of 300 K into this system, $l_{\rm sf}$ is reduced to its saturation value, α is unchanged, while ρ increases to a value which is larger than the resistivity from interface mixing only or from thermal disorder only. This suggests that for $Co_1|Ni_2$ multilayers, both $l_{\rm sf}$ and α tend to saturate with increasing disorder, whereas ρ continues to increase as more disorder is introduced.

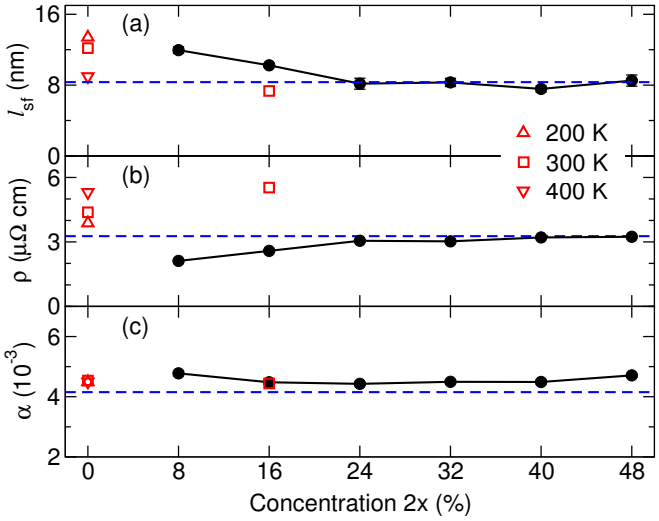

FIG. 2. (a) Calculated spin-flip diffusion length $l_{\rm sf}$, (b) resistivity ρ and (c) Gilbert damping parameter α as functions of the interface mixing in $Co_1|Ni_2$ multilayers. The mixing is characterized by the concentration $2x$ of Ni atoms in the Co layer and the corresponding system is $Co_{1-2x}Ni_{2x}|Ni_{2(1-x)}Co_{2x}$. The values calculated with frozen thermal lattice disorder are included for comparison. At $2x$=16%, we combine interface mixing and frozen thermal lattice disorder corresponding to 300 K. The dashed lines show the corresponding values for a homogeneous $Co_{33}Ni_{67}$ alloy at zero temperature.

TABLE III. Calculated Gilbert damping parameter of magnetic MLs with CPP geometry.

α ($\times 10^{-3}$)	200 K	300 K	400 K
$Co_1|Cu_2$	4.81±0.10	4.42±0.08	4.50±0.12
$\alpha_\parallel$	6.23±0.15	5.67±0.12	5.77±0.15
$\alpha_\perp$	3.44±0.09	3.18±0.06	3.22±0.11
$Co_1|Ni_2$	4.49±0.06	4.54±0.07	4.50±0.07
$Co_1|Pd_2$	5.34±0.24	5.63±0.10	6.25±0.13
$Co_1|Pt_2$	69.06±1.32	61.59±1.62	56.65±1.13
$Co_1|Ni_5$	8.05±0.12	7.90±0.07	7.87±0.13

IV. SUMMARY

We report the results of first-principles calculations of the spin-flip diffusion length $l_{\rm sf}$, resistivity ρ and Gilbert damping α with frozen thermal lattice disorder for $Co_1|X_2$ (X=Cu, Ni, Pd, Pt) and $Co_1|Ni_5$ magnetic MLs in the framework of scattering theory. $l_{\rm sf}$ decreases and ρ increases with increasing thermal disorder

in all systems. α for $Co_1|Ni_2$ ML has little temperature dependence and does not increase with additional interface mixing, but increases with increasing Ni concentration, from $Co_1|Ni_2$ to $Co_1|Ni_5$. The damping for $Co_1|X_2$ (X=Cu, Pd, Pt) MLs exhibits different temperature dependences because the damping of bulk Co is modulated differently by X depending on the strength of the X spin-orbit coupling. The way in which spin-orbit coupling gives rise to large magnetic anisotropy in Co|Ni, Co|Pd and Co|Pt multilayers is not reflected in a one-to-one fashion in the values of properties such as the spin-diffusion length and the damping parameter. For example, there is no significant difference in the values the parameters l_{sf} and α have for $Co_1|Cu_2$ and $Co_1|Ni_2$ even though $Co_1|Ni_2$ has a much larger PMA. Additional calculations and more analysis are needed to understand why these results are as they are and in order to guide experimental work.

ACKNOWLEDGMENTS

This work is part of the research programmes of "Stichting voor Fundamenteel Onderzoek der Materie" (FOM) and the use of supercomputer facilities was sponsored by the "Stichting Nationale Computer Faciliteiten" (NCF), both financially supported by the "Nederlandse Organisatie voor Wetenschappelijk Onderzoek" (NWO). It was also supported by EU FP7 ICT Grant No. 251759 MACALO and Contract No. NMP3-SL-2009-233513 MONAMI.

[1] in *Ultrathin Magnetic Structures I-IV*, edited by J. A. C. Bland and B. Heinrich (Springer-Verlag, Berlin, 1994-2005).
[2] J. C. Slonczewski, J. Magn. & Magn. Mater. **159**, L1 (1996).
[3] L. Berger, Phys. Rev. B **54**, 9353 (1996).
[4] M. Tsoi, A. G. M. Jansen, J. Bass, W.-C. Chiang, M. Seck, V. Tsoi, and P. Wyder, Phys. Rev. Lett. **80**, 4281 (1998).
[5] J. Z. Sun, J. Magn. & Magn. Mater. **202**, 157 (1999).
[6] J.-E. Wegrowe, D. Kelly, Y. Jaccard, P. Guittienne, and J. P. Ansermet, Europhys. Lett. **45**, 626 (1999).
[7] E. B. Myers, D. C. Ralph, J. A. Katine, R. N. Louie, and R. A. Buhrman, Science **285**, 867 (1999).
[8] J. A. Katine, F. J. Albert, R. A. Buhrman, E. B. Myers, and D. C. Ralph, Phys. Rev. Lett. **84**, 3149 (2000).
[9] J. Grollier, A. H. V. Cros, J. M. George, H. Jaffrès, A. Fert, G. Faini, J. B. Youssef, and H. Legall, Appl. Phys. Lett. **78**, 3663 (2001).
[10] M. Tsoi, A. G. M. Jansen, J. Bass, W.-C. Chiang, V. Tsoi, and P. Wyder, Nature **406**, 46 (2000).
[11] S. I. Kiselev, J. C. Sankey, I. N. Krivorotov, N. C. Emley, R. J. Schoelkopf, R. A. Buhrman, and D. C. Ralph, Nature **425**, 380 (2003).
[12] J. Åkerman, Science **308**, 508 (2005).
[13] M. H. Kryder and C. S. Kim, IEEE Trans. Mag. **45**, 3406 (2009).
[14] A. Slavin, Nature Nanotechnology **4**, 479 (2009).
[15] S. Mangin, D. Ravelosona, J. A. Katine, M. J. Carey, B. D. Terris, and E. E. Fullerton, Nature Materials **5**, 210 (2006).
[16] D. Houssameddine, U. Ebels, B. Delaët, B. Rodmacq, I. Firastrau, F. Ponthenier, M. Brunet, C. Thirion, J.-P. Michel, L. Prejbeanu-Buda, M.-C. Cyrille, O. Redon, and B. Dieny, Nature Materials **6**, 447 (2007).
[17] A. Barman, S. Wang, O. Hellwig, A. Berger, E. E. Fullerton, and H. Schmidt, J. Appl. Phys. **101**, 09D102 (2007).
[18] S. Mangin, Y. Henry, D. Ravelosona, J. A. Katine, and E. E. Fullerton, Appl. Phys. Lett. **94**, 012502 (2009).
[19] C. Burrowes, A. P. Mihai, D. Ravelosona, J.-V. Kim, C. Chappert, L. Vila, A. Marty, Y. Samson, F. Garcia-Sanchez, L. D. Buda-Prejbeanu, I. Tudosa, E. E. Fullerton, and J.-P. Attané, Nature Physics **6**, 17 (2010).
[20] J.-M. Beaujour, D. Ravelosona, I. Tudosa, E. E. Fullerton, and A. D. Kent, Phys. Rev. B **80**, 180415 (2009).
[21] J.-M. Beaujour, A. D. Kent, D. Ravelosona, I. Tudosa, and E. E. Fullerton, J. Appl. Phys. **109**, 033917 (2011).
[22] A. A. Starikov, P. J. Kelly, A. Brataas, Y. Tserkovnyak, and G. E. W. Bauer, Phys. Rev. Lett. **105**, 236601 (2010).
[23] Y. Liu, A. A. Starikov, Z. Yuan, and P. J. Kelly, Phys. Rev. B **84**, 014412 (2011).
[24] G. H. O. Daalderop, P. J. Kelly, and M. F. H. Schuurmans, Phys. Rev. B **42**, 7270 (1990); Phys. Rev. B **44**, 12054 (1991); in *Science and Technology of Nanostructured Magnetic Materials*, NATO Advanced Science Institutes Series, Series B, Vol. 259, edited by G. Hadjipanayis and G. Prinz (Plenum, New York, U.S.A., 1991) pp. 185–190; Phys. Rev. B **50**, 9989 (1994).
[25] G. H. O. Daalderop, P. J. Kelly, and F. J. A. den Broeder, Phys. Rev. Lett. **68**, 682 (1992).
[26] M. T. Johnson, P. J. H. Bloemen, F. J. A. den Broeder, and J. J. de Vries, Rep. Prog. Phys. **59**, 1409 (1996).
[27] I. M. Miron, G. Gaudin, S. Auffret, B. Rodmacq, A. Schuhl, S. Pizzini, J. Vogel, and P. Gambardella, Nature Materials **9**, 230 (2010).
[28] T. Koyama, D. Chiba, K. Ueda, K. Kondou, H. Tanigawa, S. Fukami, T. Suzuki, N. Ohshima, N. Ishiwata, Y. Nakatani, K. Kobayashi, and T. Ono, Nature Materials **10**, 194 (2011).
[29] T. L. Gilbert, Phys. Rev. **100**, 1243 (1955), [Abstract only; full report, Armor Research Foundation Project No. A059, Supplementary Report, May 1, 1956]; IEEE Trans. Mag. **40**, 3443 (2004).
[30] D. Steiauf and M. Fähnle, Phys. Rev. B **72**, 064450 (2005).
[31] P. C. van Son, H. van Kempen, and P. Wyder, Phys. Rev. Lett. **58**, 2271 (1987).
[32] T. Valet and A. Fert, Phys. Rev. B **48**, 7099 (1993).
[33] A. Brataas, Y. Tserkovnyak, and G. E. W. Bauer, Phys. Rev. Lett. **101**, 037207 (2008).
[34] K. Xia, P. J. Kelly, G. E. W. Bauer, I. Turek, J. Kudrnovský, and V. Drchal, Phys. Rev. B **63**, 064407 (2001); K. Xia, M. Zwierzycki, M. Talanana, P. J. Kelly, and G. E. W. Bauer, Phys. Rev. B **73**, 064420 (2006).
[35] O. K. Andersen, Phys. Rev. B **12**, 3060 (1975).

[36] O. K. Andersen, Z. Pawlowska, and O. Jepsen, Phys. Rev. B **34**, 5253 (1986).

[37] I. Turek, V. Drchal, J. Kudrnovský, M. Šob, and P. Weinberger, *Electronic Structure of Disordered Alloys, Surfaces and Interfaces* (Kluwer, Boston-London-Dordrecht, 1997).

[38] The experimental lattice constants for bulk fcc Co, Ni, and Cu are a_{Co}=3.549 Å, a_{Ni}=3.524 Å, and a_{Cu}=3.614 Å.

[39] G. Kresse and J. Furthmüller, Phys. Rev. B **54**, 11169 (1996).

[40] G. Kresse and J. Furthmüller, Comp. Mat. Sci. **6**, 15 (1996).

[41] G. Kresse and D. Joubert, Phys. Rev. B **59**, 1758 (1999).

[42] The calculated lattice constants of fcc Pd and Pt are $a_{\mathrm{Pd}} = 3.96$ Å and $a_{\mathrm{Pt}} = 3.98$ Å, respectively. The calculated layer distances are $c_{\mathrm{Co\text{-}Pd}} = 2.06$ Å and $c_{\mathrm{Pd\text{-}Pd}} = 2.36$ Å for Co_1Pd_2, and $c_{\mathrm{Co\text{-}Pt}} = 2.06$ Å and $c_{\mathrm{Pt\text{-}Pt}} = 2.40$ Å for Co_1Pt_2, respectively. Relaxed multilayer structures were constructed in a similar fashion in Ref. 24.

[43] S. Baroni, P. Giannozzi, and A. Testa, Phys. Rev. Lett. **58**, 1861 (1987).

[44] K. M. Schep, J. B. A. N. van Hoof, P. J. Kelly, G. E. W. Bauer, and J. E. Inglesfield, Phys. Rev. B **56**, 10805 (1997).

[45] J. Bass and W. P. Pratt Jr., J. Phys.: Condens. Matter **19**, 183201 (2007).

[46] O. K. Andersen, O. Jepsen, and D. Glötzel, in *Highlights of Condensed Matter Theory*, International School of Physics 'Enrico Fermi', Varenna, Italy,, edited by F. Bassani, F. Fumi, and M. P. Tosi (North-Holland, Amsterdam, 1985) pp. 59–176.

[47] S. M. Bhagat and P. Lubitz, Phys. Rev. B **10**, 179 (1974).

[48] K. Gilmore, Y. U. Idzerda, and M. D. Stiles, Phys. Rev. Lett. **99**, 027204 (2007).

[49] K. Gilmore, Y. U. Idzerda, and M. D. Stiles, J. Appl. Phys. **103**, 07D303 (2008).

Ab Initio Calculation of the Gilbert Damping Parameter via the Linear Response Formalism

H. Ebert, S. Mankovsky, and D. Ködderitzsch
University of Munich, Department of Chemistry, Butenandtstrasse 5-13, D-81377 Munich, Germany

P. J. Kelly
Faculty of Science and Technology and MESA$^+$ Institute for Nanotechnology, University of Twente, P.O. Box 217, 7500 AE Enschede, The Netherlands

(Received 1 March 2011; published 2 August 2011)

A Kubo-Greenwood-like equation for the Gilbert damping parameter α is presented that is based on the linear response formalism. Its implementation using the fully relativistic Korringa-Kohn-Rostoker band structure method in combination with coherent potential approximation alloy theory allows it to be applied to a wide range of situations. This is demonstrated with results obtained for the bcc alloy system $Fe_{1-x}Co_x$ as well as for a series of alloys of Permalloy with 5*d* transition metals. To account for the thermal displacements of atoms as a scattering mechanism, an alloy-analogy model is introduced. The corresponding calculations for Ni correctly describe the rapid change of α when small amounts of substitutional Cu are introduced.

DOI: 10.1103/PhysRevLett.107.066603 PACS numbers: 72.25.Rb, 71.20.Be, 71.70.Ej, 75.78.−n

The magnetization dynamics that is relevant for the performance of any type of magnetic device is in general governed by damping. In most cases the magnetization dynamics can be modeled successfully by means of the Landau-Lifshitz-Gilbert (LLG) equation [1] that accounts for damping in a phenomenological way. The possibility to calculate the corresponding damping parameter from first principles would open the perspective of optimizing materials for devices and has therefore motivated extensive theoretical work in the past. This led among others to Kambersky's breathing Fermi surface (BFS) [2] and torque-correlation models (TCM) [3], that in principle provide a firm basis for numerical investigations based on electronic structure calculations [4,5]. The spin-orbit coupling that is seen as a key factor in transferring energy from the magnetization to the electronic degrees of freedom is explicitly included in these models. Most *ab initio* results have been obtained for the BFS model though the torque-correlation model makes fewer approximations [4,6]. In particular, it in principle describes the physical processes responsible for Gilbert damping over a wide range of temperatures as well as chemical (alloy) disorder. However, in practice, like many other models it depends on a relaxation time parameter τ that describes the rate of transfer due to the various types of possible scattering mechanisms. This weak point could be removed recently by Brataas *et al.* [7] who described the Gilbert damping by means of scattering theory. This development supplied the formal basis for the first parameter-free investigations on disordered alloys for which the dominant scattering mechanism is potential scattering caused by chemical disorder [8] or temperature induced structure disorder [9].

As pointed out by Brataas *et al.* [7], their approach is completely equivalent to a formulation in terms of the linear response or Kubo formalism. The latter route is taken in this communication that presents a Kubo-Greenwood-like expression for the Gilbert damping parameter. Application of the scheme to disordered alloys demonstrates that this approach is indeed fully equivalent to the scattering theory formulation of Brataas *et al.* [7]. In addition a scheme is introduced to deal with the temperature dependence of the Gilbert damping parameter.

Following Brataas *et al.* [7], the starting point of our scheme is the Landau-Lifshitz-Gilbert (LLG) equation for the time derivative of the magnetization $\vec{M}$:

$$\frac{1}{\gamma}\frac{d\vec{M}}{d\tau} = -\vec{M}\times\vec{H}_{\mathrm{eff}} + \vec{M}\times\left[\frac{\tilde{G}(\vec{M})}{\gamma^2 M_s^2}\frac{d\vec{M}}{d\tau}\right], \qquad (1)$$

where M_s is the saturation magnetization, γ the gyromagnetic ratio, and $\tilde{G}$ the Gilbert damping tensor. Accordingly, the time derivative of the magnetic energy is given by

$$\dot{E}_{\mathrm{mag}} = \vec{H}_{\mathrm{eff}}\cdot\frac{d\vec{M}}{d\tau} = \frac{1}{\gamma^2}\dot{\vec{m}}[\tilde{G}(\vec{m})\dot{\vec{m}}] \qquad (2)$$

in terms of the normalized magnetization $\vec{m} = \vec{M}/M_s$. On the other hand, the energy dissipation of the electronic system $\dot{E}_{\mathrm{dis}} = \langle\frac{d\hat{H}}{d\tau}\rangle$ is determined by the underlying Hamiltonian $\hat{H}(\tau)$. Expanding the normalized magnetization $\vec{m}(\tau)$, that determines the time dependence of $\hat{H}(\tau)$ about its equilibrium value, $\vec{m}(\tau) = \vec{m}_0 + \vec{u}(\tau)$, one has

$$\hat{H} = \hat{H}_0(\vec{m}_0) + \sum_\mu \vec{u}_\mu\frac{\partial}{\partial\vec{u}_\mu}\hat{H}(\vec{m}_0). \qquad (3)$$

Using the linear response formalism, $\dot{E}_{\mathrm{dis}}$ can be written as [7]

$$\dot{E}_{\mathrm{dis}} = -\pi\hbar \sum_{ii'} \sum_{\mu\nu} \dot{u}_\mu \dot{u}_\nu \left\langle \psi_i \left| \frac{\partial \hat{H}}{\partial u_\mu} \right| \psi_{i'} \right\rangle \left\langle \psi_{i'} \left| \frac{\partial \hat{H}}{\partial u_\nu} \right| \psi_i \right\rangle \times \delta(E_F - E_i)\delta(E_F - E_{i'}), \quad (4)$$

where E_F is the Fermi energy and the sums run over all eigenstates α of the system. Identifying $\dot{E}_{\mathrm{mag}} = \dot{E}_{\mathrm{dis}}$, one gets an explicit expression for the Gilbert damping tensor $\tilde{G}$ or equivalently for the damping parameter $\alpha = \tilde{G}/(\gamma M_s)$ [7]. In full analogy to electric transport [10], the sum over eigenstates $|\psi_i\rangle$ may be expressed in terms of the retarded single-particle Green's function $\mathrm{Im}G^+(E_F) = -\pi \sum_i |\psi_i\rangle\langle\psi_i| \delta(E_F - E_i)$. This leads for the parameter α to a Kubo-Greenwood-like equation

$$\alpha_{\mu\nu} = -\frac{\hbar\gamma}{\pi M_s} \mathrm{Trace} \left\langle \frac{\partial \hat{H}}{\partial u_\mu} \mathrm{Im}G^+(E_F) \frac{\partial \hat{H}}{\partial u_\nu} \mathrm{Im}G^+(E_F) \right\rangle_c \quad (5)$$

with $\langle \ldots \rangle_c$ indicating a configurational average in case of a disordered system (see below). Identifying $T_\mu = \partial \hat{H}/\partial u_\mu$ with the component of the magnetic torque operator $\hat{\vec{I}}$ along the direction $\vec{n}$, such that $\hat{I}_{\vec{n}} = \partial \hat{H}/\partial \vec{u}(\vec{n} \times \vec{u}) = \partial \hat{H}/\partial u_\mu (\vec{n} \times \vec{u})_\mu$ this expression obviously gives the parameter α in terms of a torque-torque correlation function. However, in contrast to the conventional TCM the electronic structure is not represented in terms of Bloch states but using the retarded electronic Green's function giving the present approach much more flexibility.

The most reliable way to account for spin-orbit coupling as the source of Gilbert damping is to evaluate Eq. (5) using a fully relativistic Hamiltonian within the framework of local spin density formalism (LSDA) [11]:

$$\hat{H} = c\vec{\alpha}\,\vec{p} + \beta mc^2 + V(\vec{r}) + \beta\vec{\sigma}\,\vec{m}\,B(\vec{r}). \quad (6)$$

Here α_i and β are the standard Dirac matrices and $\vec{p}$ is the relativistic momentum operator [12]. The functions V and B are the spin-averaged and spin-dependent parts, respectively, of the LSDA potential. Equation (6) implies for the T_μ operator occurring in Eq. (5) the expression

$$T_\mu = \frac{\partial}{\partial u_\mu} \hat{H} = \beta B \sigma_\mu. \quad (7)$$

The Green's function G^+ in Eq. (5) can be obtained in a very efficient way by using the spin-polarized relativistic version of multiple scattering theory [11] that allows us to treat magnetic solids:

$$G^+(\vec{r}_n, \vec{r}'_m, E) = \sum_{\Lambda\Lambda'} Z^n_\Lambda(\vec{r}_n, E) \tau^{nm}_{\Lambda\Lambda'}(E) Z^{m\times}_{\Lambda'}(\vec{r}'_m, E) - \sum_\Lambda Z^n_\Lambda(\vec{r}_<, E) J^{n\times}_{\Lambda'}(\vec{r}_>, E) \delta_{nm}. \quad (8)$$

Here coordinates $\vec{r}_n$ referred to the center of cell n have been used with $|\vec{r}_<| = \min(|\vec{r}_n|, |\vec{r}'_n|)$ and $|\vec{r}_>| = \max(|\vec{r}_n|, |\vec{r}'_n|)$. The four-component wave functions $Z^n_\Lambda(\vec{r}, E)$ ($J^n_\Lambda(\vec{r}, E)$) are regular (irregular) solutions to the single-site Dirac equation for site n and $\tau^{nm}_{\Lambda\Lambda'}(E)$ is the so-called scattering path operator that transfers an electronic wave coming in at site m into a wave going out from site n with all possible intermediate scattering events accounted for coherently.

Using matrix notation, this leads to the following expression for the damping parameter:

$$\alpha_{\mu\mu} = \frac{g}{\pi\mu_{\mathrm{tot}}} \sum_n \mathrm{Trace} \langle \underline{T}^{0\mu} \underline{\tilde{\tau}}^{0n} \underline{T}^{n\mu} \underline{\tilde{\tau}}^{n0} \rangle_c \quad (9)$$

with the g factor $2(1 + \mu_{\mathrm{orb}}/\mu_{\mathrm{spin}})$ in terms of the spin and orbital moments, μ_{spin} and μ_{orb}, respectively, the total magnetic moment $\mu_{\mathrm{tot}} = \mu_{\mathrm{spin}} + \mu_{\mathrm{orb}}$, and $\tilde{\tau}^{0n}_{\Lambda\Lambda'} = \frac{1}{2i}(\tau^{0n}_{\Lambda\Lambda'} - \tau^{0n}_{\Lambda'\Lambda})$ and with the energy argument E_F omitted. The matrix elements of the torque operator, $\underline{T}^{n\mu}$, are identical to those occurring in the context of exchange coupling [13] and can be expressed in terms of the spin-dependent part B of the electronic potential with matrix elements:

$$T^{n\mu}_{\Lambda'\Lambda} = \int d^3r Z^{n\times}_{\Lambda'}(\vec{r}) [\beta\sigma_\mu B_{xc}(\vec{r})] Z^n_\Lambda(\vec{r}). \quad (10)$$

As indicated above, the expressions in Eqs. (5)–(10) can be applied straightforwardly to disordered alloys. In this case the brackets $\langle \ldots \rangle_c$ indicate the necessary configurational average. This can be done by describing in a first step the underlying electronic structure (for $T = 0$ K) on the basis of the coherent potential approximation (CPA) alloy theory. In the next step the configurational average in Eq. (5) is taken following the scheme worked out by Butler [10] when dealing with the electrical conductivity at $T = 0$ K or residual resistivity, respectively, of disordered alloys. This implies, in particular, that so-called vertex corrections of the type $\langle T_\mu \mathrm{Im}G^+ T_\nu \mathrm{Im}G^+ \rangle_c - \langle T_\mu \mathrm{Im}G^+ \rangle_c \langle T_\nu \mathrm{Im}G^+ \rangle_c$ that account for scattering-in processes in the language of the Boltzmann transport formalism are properly accounted for.

Thermal vibrations as a source of electron scattering can in principle be accounted for by a generalization of Eqs. (5)–(10) to finite temperatures and by including the electron-phonon self-energy $\Sigma_{\text{el-ph}}$ when calculating the Green's function G^+. Here we restrict ourselves to elastic scattering processes by using a quasistatic representation of the thermal displacements of the atoms from their equilibrium positions. We introduce an alloy-analogy model to average over a discrete set of displacements that is chosen to reproduce the thermal root mean square average displacement $\sqrt{\langle u^2 \rangle_T}$ for a given temperature T. This was chosen according to $\langle u^2 \rangle_T = \frac{1}{4} \frac{3h^2}{\pi^2 mk\Theta_D} \left[\frac{\Phi(\Theta_D/T)}{\Theta_D/T} + \frac{1}{4} \right]$ with $\Phi(\Theta_D/T)$ the Debye function, h the Planck constant, k the Boltzmann constant, and Θ_D the Debye temperature [14]. Ignoring the zero temperature term $1/4$ and assuming a frozen potential for the atoms, the situation can be dealt

with in full analogy to the treatment of disordered alloys described above.

The approach described above has been applied to the ferromagnetic 3*d*-transition metal alloy systems bcc $Fe_{1-x}Co_x$, fcc $Fe_{1-x}Ni_x$, and fcc $Co_{1-x}Ni_x$. Figure 1 shows as an example results for bcc $Fe_{1-x}Co_x$ for $x \leq 0.7$. The calculated damping parameter $\alpha(x)$ for $T = 0$ K is found to be in very good agreement with the results based on the scattering theory approach [8] demonstrating numerically the equivalence of the two approaches. An indispensable requirement to achieving this agreement is to include the vertex corrections mentioned above. In fact, ignoring them leads in some cases to completely unphysical results. To check the reliability of the standard CPA, that implies a single-site approximation when performing the configurational average, we performed calculations on the basis of the nonlocal CPA [15]. Using a four-atom cluster led to practically the same results as the CPA except for the very dilute case. As found before for fcc $Fe_{1-x}Ni_x$ [8] the theoretical results for α reproduce the concentration dependence of the experimental data quite well but are found to be too low (see below). As suggested by Eq. (9) the variation of $\alpha(x)$ with concentration x may reflect to some extent the variation of the average magnetic moment of the alloy, μ_{tot}. Because the moments and spin-orbit coupling strength do not differ very much for Fe and Co, the variation of $\alpha(x)$ should be determined in the concentrated regime primarily by the electronic structure at the Fermi energy E_F. As Fig. 1 shows, there is indeed a close correlation with the density of states $n(E_F)$ that may be seen as a measure for the number of available relaxation channels.

While the scattering and linear response approach are completely equivalent when dealing with bulk alloys the latter allows us to perform the necessary configuration averaging in a much more efficient way. This allows us to study with moderate effort the influence of varying the alloy composition on the damping parameter α. Corresponding work has been done, in particular, using Permalloy as a starting material and adding transition metals (TM) [16] or rare earth metals [17]. If we use the present scheme to study the effect of substituting Fe and Ni atoms in Permalloy with a 5*d* TM, we find an increase of α nearly linear with the 5*d* TM content, just as in experiment [16]. The total damping for 10% 5*d* TM content shown in Fig. 2 (top) varies roughly parabolically over the 5*d* TM series. In contrast to the $Fe_{1-x}Co_x$ alloys considered above, there is now an *S*-like variation of the moments μ_{spin}^{5d} over the series (Fig. 2, bottom), characteristic of 5*d* impurities in the pure hosts Fe and Ni [18,19]. In spite of this behavior of μ_{spin}^{5d} the variation of $\alpha(x)$ seems again to be correlated with the density of states $n^{5d}(E_F)$ (Fig. 2 bottom). Again the trend of the experimental data is well reproduced by the calculated values that are, however, somewhat too low.

One possible reason for the discrepancy between the theoretical and experimental results shown in Figs. 1 and 2 might be the neglect of the influence of finite temperatures. This can be included as indicated above to account for the thermal displacement of the atoms in a quasistate way by performing a configurational average over the displacements using the CPA. This leads even for pure systems to a scattering mechanism and this way to a finite value for α. Corresponding results for pure Ni are given in Fig. 3 that show in full accordance with experiment a rapid decrease of α with increasing temperature until a regime with a weak variation of α with T is reached. This behavior is commonly interpreted as a transition from conductivitylike to resistivitylike behavior reflecting the dominance of intra- and interband transition, respectively [4], that is related to the increase of the broadening of electron energy bands caused by the increase of scattering events with temperature. Adding even less than 1 at. % Cu to Ni strongly reduces the conductivitylike behavior at low temperatures while leaving the high-temperature behavior essentially unchanged. A further increase of the Cu content leads to the impurity-scattering processes responsible for

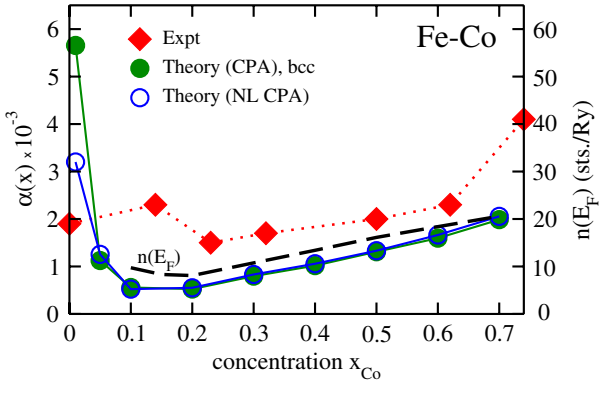

FIG. 1 (color online). Gilbert damping parameter for bcc $Fe_{1-x}Co_x$ as a function of Co concentration: full circles—the present results within CPA; empty circles—within nonlocal CPA (NL CPA); and full diamonds—experimental data by Oogane [20].

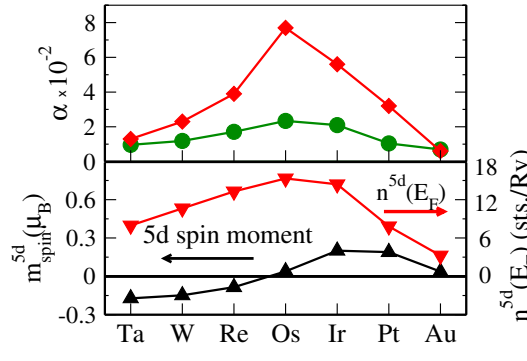

FIG. 2 (color online). Top: Gilbert damping parameter α for Py/5*d* TM systems with 10% 5*d* TM content in comparison with experiment [16]; bottom: spin magnetic moment m_{spin}^{5d} and density of states $n(E_F)$ at the Fermi energy of the 5*d* component in Py/5*d* TM systems with 10% 5*d* TM content.

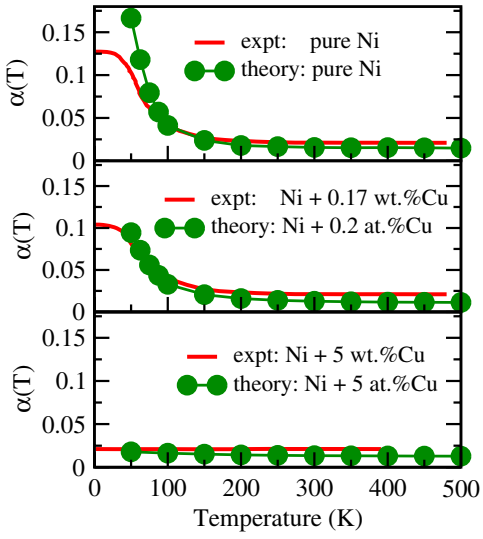

FIG. 3 (color online). Temperature variation of Gilbert damping of pure Ni and Ni with Cu impurities: present theoretical results vs experiment [21].

band broadening dominating α. This effect completely suppresses the conductivitylike behavior in the low-temperature regime because of the increase of scattering events due to chemical disorder. Again this is fully in line with the experimental data, providing a straightforward explanation for their peculiar variation with temperature and composition.

From the results obtained for Ni one may conclude that thermal lattice displacements are only partly responsible for the finding that the damping parameters obtained for Py doped with the 5*d* TM series, and $Fe_{1-x}Co_x$ are somewhat low compared with experiment. This indicates that additional relaxation mechanisms like magnon scattering contribute. Again, these can be included at least in a quasistatic way by adopting the point of view of a disordered local moment picture. This implies scattering due to random temperature-dependent fluctuations of the spin moments that can also be dealt with using the CPA.

In summary, a formulation for the Gilbert damping parameter α in terms of a torque-torque-correlation function was derived that led to a Kubo-Greenwood-like equation. The scheme was implemented using the fully relativistic Korringa-Kohn- Rostoker band structure method in combination with the CPA alloy theory. This allows us to account for various types of scattering mechanisms in a parameter-free way. Corresponding applications to disordered transition metal alloys led to very good agreement with results based on the scattering theory approach of Brataas *et al.* demonstrating the equivalence of both approaches. The flexibility and numerical efficiency of the present scheme was demonstrated by a study on a series of Permalloy-5*d* TM systems. To investigate the influence of finite temperatures on α, a so-called alloy-analogy model was introduced that deals with the thermal displacement of atoms in a quasistatic manner. Applications to pure Ni gave results in very good agreement with experiment and, in particular, reproduced the dramatic change of α when Cu is added to Ni.

The authors would like to thank the DFG for financial support within the SFB 689 "Spinphänomene in reduzierten Dimensionen" and within project Eb154/23 for financial support. P. J. K acknowledges support by EU FP7 ICT Grant No. 251759 MACALO.

[1] T. L. Gilbert, IEEE Trans. Magn. **40**, 3443 (2004).
[2] V. Kambersky, Can. J. Phys. **48**, 2906 (1970).
[3] V. Kambersky, Czech. J. Phys. **26**, 1366 (1976).
[4] K. Gilmore, Y. U. Idzerda, and M. D. Stiles, Phys. Rev. Lett. **99**, 027204 (2007).
[5] M. Fähnle and D. Steiauf, Phys. Rev. B **73**, 184427 (2006).
[6] V. Kambersky, Phys. Rev. B **76**, 134416 (2007).
[7] A. Brataas, Y. Tserkovnyak, and G. E. W. Bauer, Phys. Rev. Lett. **101**, 037207 (2008).
[8] A. A. Starikov, P. J. Kelly, A. Brataas, Y. Tserkovnyak, and G. E. W. Bauer, Phys. Rev. Lett. **105**, 236601 (2010).
[9] Y. Liu, A. A. Starikov, Z. Yuan, and P. J. Kelly, Phys. Rev. B **84**, 014412 (2011).
[10] W. H. Butler, Phys. Rev. B **31**, 3260 (1985).
[11] H. Ebert, in *Electronic Structure and Physical Properties of Solids*, edited by H. Dreyssé, Lecture Notes in Physics Vol. 535 (Springer, Berlin, 2000), p. 191.
[12] M. E. Rose, *Relativistic Electron Theory* (Wiley, New York, 1961).
[13] H. Ebert and S. Mankovsky, Phys. Rev. B **79**, 045209 (2009).
[14] E. M. Gololobov, E. L. Mager, Z. V. Mezhevich, and L. K. Pan, Phys. Status Solidi (b) **119**, K139 (1983).
[15] D. Ködderitzsch, H. Ebert, D. A. Rowlands, and A. Ernst, New J. Phys. **9**, 81 (2007).
[16] J. O. Rantschler, R. D. McMichael, A. Castillo, A. J. Shapiro, W. F. Egelhoff, B. B. Maranville, D. Pulugurtha, A. P. Chen, and L. M. Connors, J. Appl. Phys. **101**, 033911 (2007).
[17] G. Woltersdorf, M. Kiessling, G. Meyer, J.-U. Thiele, and C. H. Back, Phys. Rev. Lett. **102**, 257602 (2009).
[18] B. Drittler, N. Stefanou, S. Blügel, R. Zeller, and P. H. Dederichs, Phys. Rev. B **40**, 8203 (1989).
[19] N. Stefanou, A. Oswald, R. Zeller, and P. H. Dederichs, Phys. Rev. B **35**, 6911 (1987).
[20] M. Oogane, T. Wakitani, S. Yakata, R. Yilgin, Y. Ando, A. Sakuma, and T. Miyazaki, Jpn. J. Appl. Phys. **45**, 3889 (2006).
[21] S. M. Bhagat and P. Lubitz, Phys. Rev. B **10**, 179 (1974).

First-principles calculations of magnetization relaxation in pure Fe, Co, and Ni with frozen thermal lattice disorder

Yi Liu, Anton A. Starikov, Zhe Yuan, and Paul J. Kelly

Faculty of Science and Technology and MESA$^+$ *Institute for Nanotechnology, University of Twente, P.O. Box 217, NL-7500 AE Enschede, The Netherlands*

(Received 7 February 2011; revised manuscript received 1 June 2011; published 22 July 2011)

The effect of the electron-phonon interaction on magnetization relaxation is studied within the framework of first-principles scattering theory for Fe, Co, and Ni by displacing atoms in the scattering region randomly with a thermal distribution. This "frozen thermal lattice disorder" approach reproduces the nonmonotonic damping behavior observed in ferromagnetic resonance measurements and yields reasonable quantitative agreement between calculated and experimental values. It can be readily applied to alloys and easily extended by determining the atomic displacements from *ab initio* phonon spectra.

DOI: 10.1103/PhysRevB.84.014412 PACS number(s): 75.50.Cc, 72.25.Ba, 72.25.Rb, 72.10.Di

I. INTRODUCTION

The drive to increase magnetic storage densities and reduce access times is focusing renewed attention on magnetization dynamics in response to currents and external fields.[1] The dynamics of a magnetization $\mathbf{M}$ in an effective field $\mathbf{H}_{\text{eff}}$ is usually described with the phenomenological Landau-Lifshitz-Gilbert equation

$$\frac{d\mathbf{M}}{dt} = -\gamma \mathbf{M} \times \mathbf{H}_{\text{eff}} + \mathbf{M} \times \left[\frac{\lambda(\mathbf{M})}{\gamma M_s^2} \frac{d\mathbf{M}}{dt} \right], \qquad (1)$$

where $M_s = |\mathbf{M}|$ is the saturation magnetization density and $\gamma = g\mu_0\mu_B/\hbar$ is the gyromagnetic ratio expressed in terms of the Landé g factor and the Bohr magneton μ_B. The first term describes the precessional motion of the magnetization in the effective field that includes the external applied field, the exchange field, anisotropy and demagnetization fields. The second term describes the time decay of the magnetization precession, the Gilbert damping,[2] in terms of $\lambda(\mathbf{M})$ which is, in general, a symmetric 3×3 tensor.[3] For isotropic media, the damping is frequently expressed in terms of the dimensionless parameter α given by the diagonal element of λ, $\alpha = \lambda/\gamma M_s$.

There is general agreement that spin-orbit coupling (SOC) and disorder are essential ingredients in any description of how spin excitations relax to the ground state. In the absence of any other form of disorder, one might expect the damping to increase monotonically with temperature in clean magnetic materials and indeed, this is what is observed for Fe in ferromagnetic resonance (FMR) measurements.[4,5] Heinrich *et al.*[6] developed an explicit model for this high-temperature behavior in which itinerant s electrons scatter from localized d moments and transfer spin angular momentum to the lattice via SOC. This s-d model results in a damping that is inversely proportional to the electronic relaxation time, $\alpha \sim 1/\tau$, i.e., is *resistivity*-like. However, at low temperatures, both Co and Ni exhibit a sharp rise in damping as the temperature decreases.[5,7] The so-called breathing Fermi surface model was proposed[8–10] to describe this low-temperature *conductivity*-like damping, $\alpha \sim \tau$. In this model the electronic population lags behind the instantaneous equilibrium distribution due to the precessing magnetization and requires dissipation of energy and angular momentum to bring the system back to equilibrium.

Of the numerous microscopic models that have been proposed[11] to explain the damping behavior of metals, only the so-called "torque correlation model" (TCM)[12] is qualitatively successful in explaining the nonmonotonic behavior observed for hexagonal-close-packed (hcp) Co. An effective field approach can be used[13–15] to identify conductivity-like and resistivity-like behavior at low and high temperatures, respectively, with intraband and interband terms in the TCM.[11] Evaluation of this model for Fe, Co, and Ni using first-principles calculations including SOC for the host electronic structure and a band-, wave-vector- and spin-independent relaxation time approximation (RTA) to model disorder yields results for the damping α in good qualitative and reasonable quantitative agreement with the experimental observations.[13–15] The disadvantage of the RTA is that it is difficult to unambiguously map microscopically measured disorder onto a unique value of the relaxation time τ.

A formulation of magnetization damping in terms of scattering theory, that is equivalent in linear response to the Kubo formalism,[16] was recently applied to the study of substitutional alloys with intrinsic disorder yielding good agreement with experiment without introducing any parameters.[17] The discrepancies remaining between the experimental data measured at room temperature (and higher) and the $T = 0$ calculations pose questions about the role of various types of thermal disorder. In this paper we combine the scattering theory formulation of Gilbert damping with structural lattice disorder to model finite temperature lattice effects. Our main result is to show that this can reproduce the nonmonotonic behavior of the magnetization relaxation as a function of temperature.

The paper is organized as follows. In Sec. II, the "frozen thermal lattice disorder" scheme is introduced and a brief description of the scattering theory is given. This is followed by some technical details of how the calculations are performed and how the resistivity and Gilbert damping parameter are determined. The results are presented and discussed in Sec. III and compared to previous calculations and experiments. A short summary and some concluding remarks can be found in Sec. IV. In the Appendix, we discuss a factor of 4π commonly omitted when Gilbert damping frequencies are given in Gaussian units.

II. THEORETICAL METHODS AND COMPUTATIONAL DETAILS

Assuming the Born-Oppenheimer approximation,[18] static disorder is introduced in the transport calculations by displacing atoms rigidly and randomly from their ideal lattice positions in what we call a frozen thermal lattice disorder scheme.[19] In the temperature range we are interested in, far below the melting point, typical displacements are of the order of several hundredths of an angstrom, which is small compared to the lattice constant. We can therefore adopt a harmonic approximation and corresponding Gaussian distribution of displacements characterized by the root-mean-square (rms) displacement, $\Delta = \sqrt{\langle |\mathbf{u}_i|^2 \rangle}$, where the angular brackets indicate an average in which the index i runs over all atoms (Fig. 1). As the temperature increases, higher-energy phonon modes are occupied so Δ increases. In the present study, this qualitative correlation between temperature and Δ is sufficient to produce a nonmonotonic damping. If we knew the phonon dispersion relation from a Debye model or *ab initio* calculations, the atomic displacements could be determined explicitly by summing contributions from all vibrational modes occupied at a specified temperature. Such a description of the lattice disorder introduced by finite temperatures could then be straightforwardly combined with scattering theory to study temperature-dependent magnetization relaxation quantitatively.

It was shown by Brataas *et al.*[16] that, for a single domain ferromagnetic metal (FM) sandwiched between left- and right-hand leads of nonmagnetic (NM) material, the Gilbert damping tensor $\tilde{G}$ can be expressed as

$$\tilde{G}_{i,j}(\mathbf{m}) = \lambda(\mathbf{m}) \cdot V = \frac{\gamma^2 \hbar}{4\pi} \mathrm{Re}\left\{ \mathrm{Tr}\left[\frac{\partial S}{\partial m_i} \frac{\partial S^\dagger}{\partial m_j} \right] \right\}, \quad (2)$$

where V is the volume of the ferromagnet and the scattering matrix $S = \begin{pmatrix} r & t' \\ t & r' \end{pmatrix}$ is given in terms of reflection and transmission matrices for Bloch waves incident from the left (r and t) or right (r' and t') leads. When SOC is included, S depends on the direction of the magnetization unit vector $\mathbf{m} = \mathbf{M}/M_s$. The microscopic picture of magnetization damping implicit in the scattering formulation is of energy being transferred slowly from the spin degrees of freedom through disorder scattering and SOC to the electronic orbital degrees of freedom, and then being rapidly lost to phonon degrees of freedom in thermal reservoirs attached to the leads. From the transmission matrices, we can also calculate the conductance of the system within the Landauer-Büttiker formulation as $G = (e^2/h)\mathrm{Tr}\{tt^\dagger\}$.

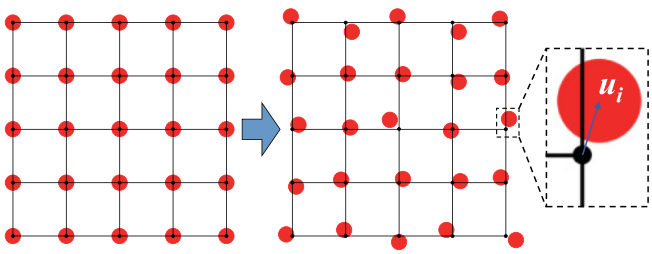

FIG. 1. (Color online) Schematic picture of the proposed frozen thermal lattice disorder. Atoms (red dots) on the ideal lattice (left panel) are displaced with a random Gaussian distribution and form a static configuration (right panel) in the electronic transport calculation. The displacement of atom i is denoted as $\mathbf{u}_i$ (blowup).

To evaluate the scattering matrix at the Fermi level, we use a "wave-function matching" scheme[20] implemented with tight-binding linearized muffin-tin orbitals (TB-LMTOs)[21] that was recently extended to include SOC.[17] The electronic structure of the NM|FM|NM sandwich is first determined self-consistently using a surface Green's function method[22] with a minimal basis of TB-LMTOs in the atomic sphere approximation. In the current study of Fe, Co, and Ni, we consider Au|Fe|Au, Cu|Co|Cu, and Cu|Ni|Cu sandwiches so the lattice constants of the NM leads and FM scattering regions match almost perfectly.[23] The two-dimensional (2D) Brillouin zone (BZ) of the 1×1 unit cell is sampled with a 120×120 grid in the self-consistent calculations.

Disorder is introduced by randomly displacing atomic spheres in the FM scattering region using the frozen thermal lattice disorder scheme described above. The calculations are rendered tractable by imposing periodic boundary conditions transverse to the transport direction. It turns out that good results can be achieved even when these so-called "lateral supercells" are quite modest in size. In practice, a 4×4 lateral supercell and a 28×28 2D BZ grid were found to be sufficient for Fe, and a 5×5 supercell and a 32×32 grid for Co and Ni, respectively.[24] The thickness of the FM region ranges from 20 to 340 atomic monolayers. For every thickness of the ferromagnet, we average over a number of random disorder configurations. The sample-to-sample spread is small for large values of Δ and five configurations are sufficient; for small values of Δ, as many as 35 configurations are used.

For a ferromagnetic slab of thickness L, we write the resistance of the system as $R(L) = 1/G(L) = 1/G_{\mathrm{Sh}} + 2R_{\mathrm{if}} + R_{\mathrm{b}}(L)$, where $G(L)$ is the total conductance, and G_{Sh} the Sharvin conductance of the ideal leads; R_{if} is the NM|FM interface resistance and $R_{\mathrm{b}}(L)$ is the bulk contribution.[20,25] When the ferromagnetic slab is sufficiently thick, we expect to recover Ohmic behavior with $R_{\mathrm{b}}(L) \approx \rho L$; this was demonstrated explicitly for the case of alloy disorder in Ref. 17. As shown in Fig. 2(a), this expectation is borne out by the present calculations and the resistivity ρ arising from the frozen thermal lattice disorder can be extracted from linear fitting. We write the damping parameter $\tilde{G}$ analogously as the sum of an interface contribution $\tilde{G}_{\mathrm{if}}$ and a bulk contribution $\tilde{G}_{\mathrm{b}}(L)$. If we further express the bulk contribution in terms of the dimensionless damping parameter α as $\tilde{G}_{\mathrm{b}}(L) = \lambda V = \alpha\gamma M_s A L$, where A is the cross section, then we expect the calculated damping to grow linearly with the thickness of the ferromagnetic layers, $\tilde{G}(L) = \tilde{G}_{\mathrm{if}} + \alpha\gamma M_s A L$. Once again, this expectation is borne out by the calculations as demonstrated in Fig. 2(b), and α can be determined from the slope.

III. RESULTS AND DISCUSSION

The resistivities and damping parameters calculated for bulk Fe, Co, and Ni are shown as a function of the rms displacement in Fig. 3. For all three materials, ρ increases monotonically with Δ, as expected, and α agrees with the

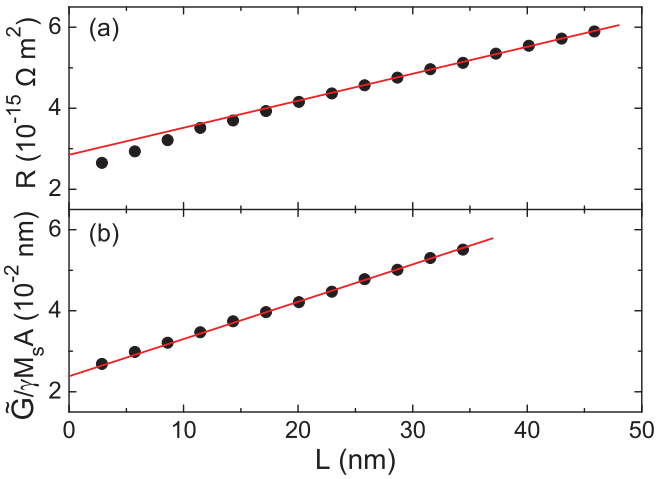

FIG. 2. (Color online) Total resistance (a) and damping (b) as functions of the thickness of the ferromagnetic slab for Au|Fe|Au(001) with $\Delta = 0.0259\, a_{\mathrm{Fe}}$. Dots indicate the calculated values averaged over five configurations while the solid line is a linear fit.

predictions of the torque correlation model.[12–14] For large values of Δ, α calculated for Fe and Co is found to increase with increasing Δ, whereas it tends to saturate for Ni, in agreement with experiment.[4,5,7] For small values of Δ, α increases rapidly as Δ decreases. This sharp rise is the conductivity-like behavior observed at low temperatures for Co and Ni, demonstrating that a simple model of frozen thermal lattice disorder can reproduce the nonmonotonic Gilbert damping seen in experiment.

Previous first-principles studies of temperature-dependent resistivity[26] only considered nonmagnetic materials. The present work uses a different methodology to study the temperature dependence of ρ for ferromagnetic metals. While there is order-of-magnitude agreement with experiment, we cannot make a rigorous comparison if we only have a qualitative knowledge of how Δ depends on temperature T. If we adopt the commonly made assumption that the effect of temperature on ρ and α can be expressed in terms of a phenomenological scattering time $\tau(T)$, i.e., $\rho(T) = \rho[\tau(T)]$ and $\alpha(T) = \alpha[\tau(T)]$, then α should have a well-defined dependence on ρ. In the present case, this amounts to assuming that our lattice disorder can be mapped onto $\tau(T) = \tau[\Delta(T)]$. We can make a first qualitative comparison by using the experimental $\rho(T)$ (Ref. 27) to indicate a number of temperatures in Fig. 3. Around these temperatures, the corresponding damping parameters behave in the same way as observed in experiment:[4,5,7] the damping for Fe has a minimum around 273 K and increases slightly at about 500 K; at 273 K, the damping for Co has increased away from its minimum value, while that for Ni has already saturated. This qualitative agreement indicates that the correlation between ρ and α is reasonably parametrized by Δ. In Table I we compare the minimum values of damping calculated as a function of Δ with the corresponding minimum values calculated within the TCM as a function of the relaxation time τ reported in Ref. 13, and also with the minimum values determined experimentally as a function of temperature.[4,5,7] We see that our minimum

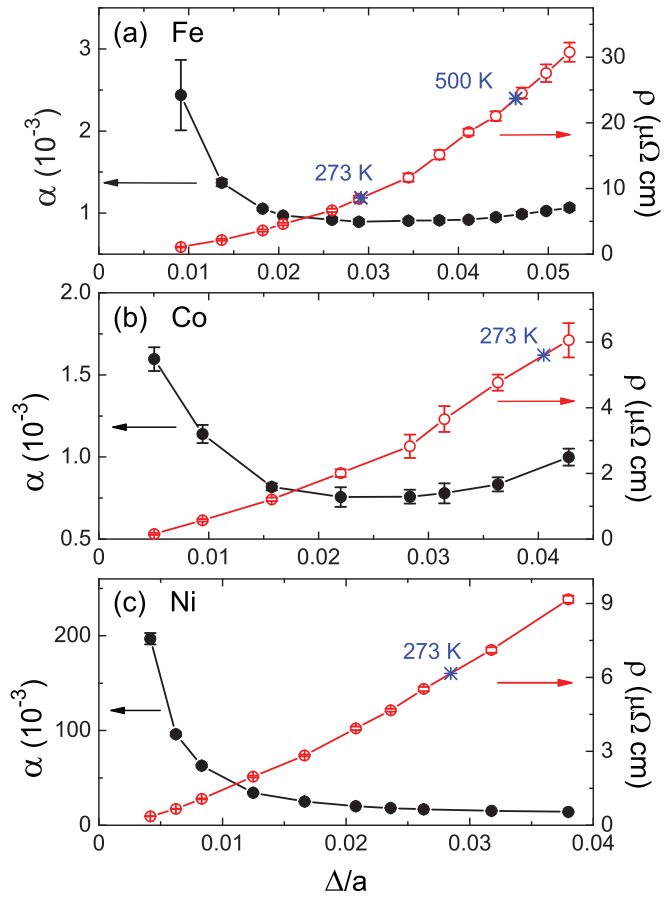

FIG. 3. (Color online) Calculated Gilbert damping and resistivity for bcc Fe, hcp Co, and fcc Ni as functions of the rms displacements measured in units of the corresponding lattice constants, a. The error bars reflect the configuration spread. Experimental resistivities (Ref. 27) are used to label a number of resistivity values with a temperature.

values are lower than the TCM values that are, in turn, lower than the experimental values.

There are two noteworthy qualitative differences between our results for small values of Δ and the low-temperature experimental observations. (i) For Fe, we find a conductivity-like damping behavior that has not been seen in experiment[4,5] but has been found in the TCM calculations.[13–15]

TABLE I. Minimum values of the Gilbert damping λ in units of 10^8 s^{-1} with respect to temperature (experiments), relaxation time τ (torque-correlation model), and Δ (present work). Experimental damping frequencies have been multiplied by 4π (see the Appendix for details).

λ	bcc Fe [001]	hcp Co [0001]	fcc Ni [111]
Experiment	8.8,[a] 4.8[b]	9[a]	29,[a] 28[c]
TCM[13]	5.4	3.7	21
This work	3.9	2.3	20

[a]Reference 5.
[b]Reference 4.
[c]Reference 7.

(ii) For Ni and Co, the saturation of the damping observed at very low temperatures[5,7] is found neither in our calculations nor in the TCM studies.[13–15] We suggest that these discrepancies are, in part, related to extrinsic contributions to the Gilbert damping that compete with the intrinsic thermal effect. There will always be some disorder in experimental samples, such as impurities and defects, whose contribution to damping is essentially temperature independent and becomes dominant when the thermal disorder becomes negligible at sufficiently low temperatures. If the extrinsic disorder in the Fe samples measured in Refs. 4 and 5 was so high that Fe was in the resistivity-like regime[28] for all temperatures, then reducing the extrinsic disorder would be expected to lower the damping. This is consistent with the minimum damping value that we calculate being smaller than the experimental value (see Table I), since our calculated damping comes only from the electron-lattice scattering, without any extrinsic contributions taken into account. For Ni and Co, which exhibit both conductivity-like and resistivity-like behavior, the discrepancies cannot be explained away so simply. Better characterization of the experimental samples, as well as further theoretical study, are required.

Comparing the minimum values of λ, as we have just done, assumes that τ (or Δ) characterizes λ and ρ completely. In particular, it assumes that the effects of various temperature-dependent disorder scattering mechanisms can be represented by a simple relaxation time. If this is correct, then the microscopic details of the disorder that gives rise to particular values of ρ and λ should not be of paramount importance and we should be able to use experimentally determined $\{\lambda(T),\rho(T)\}$ and theoretically determined $\{\lambda(\Delta),\rho(\Delta)\}$ values to compare $\lambda_{\text{expt}}(\rho)$ and $\lambda_{\text{calc}}(\rho)$. Because we are not aware of any simultaneous measurements of λ and ρ, we have combined $\lambda(T)$ and $\rho(T)$ from different experiments[4,5,7,27,29] to plot $\lambda(\rho)$ in Fig. 4; the calculated results are shown as black solid lines, while the available experimental data are shown as symbols. To facilitate the comparison, the calculated damping parameter α in Fig. 3 is converted (see the Appendix) to damping frequency λ using $\lambda = \alpha\gamma M_s$. For convenience, we have used $g = 2$ for the calculations instead of the measured g factors.

The best agreement between the calculated curve and Bhagat and Lubitz's experimental values[5] is obtained for Ni. As mentioned above, including the scattering associated with residual resistivity should *reduce* the damping calculated at low temperatures (resistivities) and increase it at high temperatures (resistivities) giving better agreement with experiment. However, it is not clear how the later measurements by Heinrich *et al.*[7] might be accommodated in this picture. Clearly, there is a need to determine which experiment most accurately represents the "intrinsic" damping in Ni. A similar situation obtains for Fe where there is an even larger discrepancy between the two existing experiments. The figure highlights the disagreement between a conductivity-like behavior at low values of resistivity in the calculations and its absence in both measurements. What is also striking is the failure of the calculations to reproduce the high-temperature (resistivity) enhancement. For Co, where there is only one measurement, we find that in a reversal of the situation for Fe the conductivity-like behavior is much more pronounced

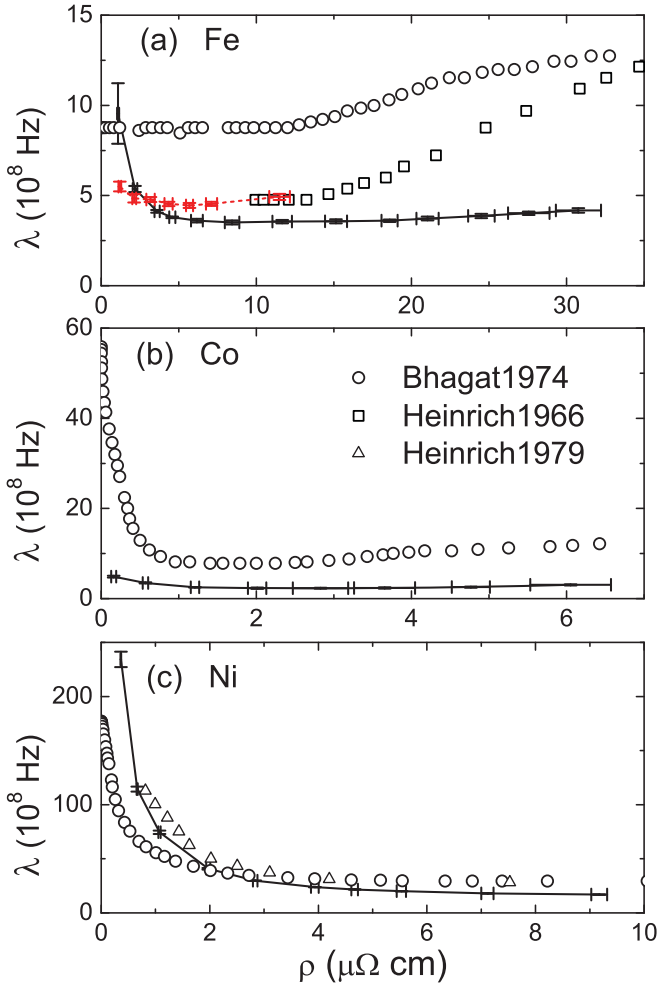

FIG. 4. (Color online) Gilbert damping frequency as a function of resistivity for bcc Fe, hcp Co, and fcc Ni. Calculated results are shown as lines: for frozen thermal lattice disorder as (black) solid lines and for frozen spin disorder as a (red) dashed line (Fe only). $g = 2$ is used in the calculations. Symbols are experimental damping values from Ref. 5 (◯), Ref. 4 (□), and Ref. 7 (△). The corresponding resistivity values are take from Refs. 27 and 29. Experimental damping frequencies have been multiplied by 4π; see the Appendix A for details.

in experiment than in our calculations. It is unclear from this and the TCM studies how much of these discrepancies might result from subtle features of the electronic structure that are described inaccurately by the local spin-density approximation. Tests with different exchange-correlation potentials and increased maximum angular momentum cutoff indicate that the corresponding changes to the electronic structure at the Fermi energy cannot explain the discrepancies.

We can test the uniqueness of τ directly by calculating $\lambda(\rho)$ for different types of disorder that give rise to the same resistivity. We do this for Fe by modeling frozen thermal spin disorder in a manner analogous to the way we have modeled frozen thermal lattice disorder. We introduce a random, Gaussian distribution of spins with respect to θ, the polar angle between the local atomic magnetization and the global magnetization directions, together with a uniform random distribution in the azimuthal angle ϕ. Together, θ and ϕ

determine the local magnetization direction. We then calculate λ and ρ as a function of the root-mean-square polar rotation angle. The results are included in Fig. 4(a) as a dashed (red) line. Although the qualitative behavior of $\lambda_{\text{lattice}}(\rho)$ and $\lambda_{\text{spin}}(\rho)$ is the same, quantitatively they are clearly different, differing by as much as a factor of 2 for the lowest value of resistivity shown. This is clear direct evidence that different microscopic scattering mechanisms contribute to resistivity and Gilbert damping differently and that it may not be sufficient to use a single electronic scattering time to represent various types of disorder. It is also of interest to study to what extent the effect of different scattering mechanisms are additive. To do so, it is desirable to introduce "real" temperatures by calculating the phonon and magnon spectra from first principles. This is a major undertaking and will be the subject of a separate study.

IV. SUMMARY AND CONCLUSIONS

In summary, we report the results of first-principles calculations of the Gilbert damping with thermal lattice disorder for pure Fe, Co, and Ni in the framework of a recently introduced scattering theory. The effect of temperature on the lattice is simulated by displacing atoms with a random, Gaussian distribution. Our main result is that both the conductivity-like and resistivity-like damping behavior observed in FMR measurements are reproduced by the scattering theory. The reasonable quantitative agreement between our results and experiment demonstrates that our simple thermal disorder scheme accounts for the dominant, intrinsic effect of lattice temperature in magnetization relaxation. By calculating the damping as a function of resistivity and comparing the results to experiment, we highlight discrepancies between different experiments and between the calculations and experiments. Part, but not all, of the discrepancies for the Gilbert damping can be attributed to competition between extrinsic and intrinsic scattering. An exploratory calculation of thermal spin disorder for Fe indicates that different types of disorder affect the Gilbert damping and resistivity in different manners. This work needs to be extended to different materials before more general conclusions can be drawn. It is of particular importance to study how different types of disorder combine to affect the damping. To avoid having to perform calculations in a two-dimensional parameter space (lattice and spin disorder), it is desirable to introduce the effect of temperature using more realistic models for the lattice and spin disorder. The method we have used can be straightforwardly extended in this direction, as well as to more complex materials. Finally, we hope that this work will stimulate more experimental temperature-dependent studies of magnetization damping.

ACKNOWLEDGMENTS

We would like to thank Arne Brataas, Yaroslav Tserkovnyak, and Gerrit Bauer for helpful discussions. This work is part of the research programs of "Stichting voor Fundamenteel Onderzoek der Materie" (FOM) and the use of supercomputer facilities was sponsored by the "Stichting Nationale Computer Faciliteiten" (NCF), both financially supported by the "Nederlandse Organisatie voor Wetenschappelijk Onderzoek" (NWO). It was also supported by EU FP7 ICT Grant No. 251759 MACALO and Contract No. NMP3-SL-2009-233513 MONAMI.

APPENDIX: 4π IN GILBERT DAMPING FREQUENCY

The damping λ has units of s^{-1} so its numerical value should not depend on whether SI or Gaussian units are used. Conversion of the dimensionless parameter α to the damping frequency λ should follow the general relation

$$\lambda = \gamma\alpha \times \text{magnetization density}. \tag{A1}$$

So, converting from SI to Gaussian units should just require converting the magnetization density M_s (magnetic moment per unit volume that we calculate as μ_B/atom) from SI to Gaussian (cgs) units.[30,31] In SI, M_s is measured in units of A/m and the damping λ is related to α by

$$\lambda = \gamma\alpha M_s \text{ (SI)}. \tag{A2}$$

In Gaussian units, the magnetization should be measured in units of magnetic moment cm^{-3}. If measured in Oersteds or Gauss, then the magnetization is $4\pi M_s$ and λ is related to α by

$$\lambda = \gamma\alpha\,(4\pi M_s) \text{ (in Gaussian units)}. \tag{A3}$$

In most experiments, the magnetization is measured and reported in Gaussian units, but Eq. (A2) is used instead of Eq. (A3), which leads to a factor 4π missing in the damping frequency.

For example, a recent measurement[32] reports the magnetization of bcc iron to be $4\pi M_s = 21.1$ kG, corresponding to 1.68×10^6 A/m in SI or 2.13 μ_B/atom. Choosing $g = 2$ (for simplicity), we have $\gamma = 0.2203$ MHz m/A$= 17.588$ MHz Oe. We convert the reported $\alpha = 0.0019$ to λ and obtain the same frequency 7.1×10^8 Hz in SI using Eq. (A2) or in Gaussian units using Eq. (A3). However, the frequency 57 ± 3 MHz reported in Ref. 32, which is obtained using Eq. (A2) combined with magnetization in Gaussian units, has to be multiplied by 4π to be consistent.

[1] See the collection of articles in *Ultrathin Magnetic Structures I–IV*, edited by J. A. C. Bland and B. Heinrich (Springer-Verlag, Berlin, 1994–2005).

[2] T. L. Gilbert, Phys. Rev. **100**, 1243 (1955) [Abstract only; full report, Armor Research Foundation Project No. A059, Supplementary Report, May 1, 1956]; T. L. Gilbert, IEEE Trans. Magn. **40**, 3443 (2004).

[3] D. Steiauf and M. Fähnle, Phys. Rev. B **72**, 064450 (2005).

[4] B. Heinrich and Z. Frait, Phys. Status Solidi B **16**, K11 (1966).

[5] S. M. Bhagat and P. Lubitz, Phys. Rev. B **10**, 179 (1974).

[6] B. Heinrich, D. Fraitová, and V. Kamberský, Phys. Status Solidi B **23**, 501 (1967).

[7] B. Heinrich, D. J. Meredith, and J. F. Cochran, J. Appl. Phys. **50**, 7726 (1979).

[8] V. Kamberský, Can. J. Phys. **48**, 1103 (1970).
[9] V. Korenman and R. E. Prange, Phys. Rev. B **6**, 2769 (1972).
[10] J. Kuneš and V. Kamberský, Phys. Rev. B **65**, 212411 (2002).
[11] B. Heinrich, in *Ultrathin Magnetic Structures III*, edited by J. A. C. Bland and B. Heinrich (Springer, New York, 2005), pp. 143–210.
[12] V. Kamberský, Czech. J. Phys. **26**, 1366 (1976).
[13] K. Gilmore, Y. U. Idzerda, and M. D. Stiles, Phys. Rev. Lett. **99**, 027204 (2007); J. Appl. Phys. **103**, 07D303 (2008).
[14] V. Kamberský, Phys. Rev. B **76**, 134416 (2007).
[15] K. Gilmore, M. D. Stiles, J. Seib, D. Steiauf, and M. Fähnle, Phys. Rev. B **81**, 174414 (2010).
[16] A. Brataas, Y. Tserkovnyak, and G. E. W. Bauer, Phys. Rev. Lett. **101**, 037207 (2008); Phys. Rev. B e-print arXiv:1104.1625v1 (to be published).
[17] A. A. Starikov, P. J. Kelly, A. Brataas, Y. Tserkovnyak, and G. E. W. Bauer, Phys. Rev. Lett. **105**, 236601 (2010).
[18] In the scattering formulation, the energy loss due to Gilbert damping is related to the energy pumped into leads by the precessing magnetization. The frequency corresponding to typical Fermi velocities in metals is $\sim 10^{16}$ Hz. Typical ferromagnetic resonance measurements from which the Gilbert damping constant is extracted are carried out at frequencies $\sim 10^{10}$ Hz so that transport electrons see essentially frozen spins. Spin-wave ($\sim 10^{13}$ Hz) and phonon frequencies ($\sim 10^{12}$ Hz) are also much lower than the electronic frequencies, justifying the use of a frozen phonon approach.
[19] A similar scheme has been developed in the framework of linear response theory, implemented using the fully relativistic Korringa-Kohn-Rostoker method in combination with the coherent potential approximation, and applied to Ni by H. Ebert, S. Mankovsky, D. Ködderitzsch, and P. J. Kelly, Phys. Rev. Lett. e-print arXiv:1102.4551v1 (to be published).
[20] K. Xia, P. J. Kelly, G. E. W. Bauer, I. Turek, J. Kudrnovský, and V. Drchal, Phys. Rev. B **63**, 064407 (2001); K. Xia, M. Zwierzycki, M. Talanana, P. J. Kelly, and G. E. W. Bauer, *ibid.* **73**, 064420 (2006).
[21] O. K. Andersen, Phys. Rev. B **12**, 3060 (1975); O. K. Andersen, Z. Pawlowska, and O. Jepsen, *ibid.* **34**, 5253 (1986).
[22] I. Turek, V. Drchal, J. Kudrnovský, M. Šob, and P. Weinberger, *Electronic Structure of Disordered Alloys, Surfaces and Interfaces* (Kluwer, Boston, 1997).
[23] The lattice constant of bcc Fe is $a_{\mathrm{Fe}} = 2.867$ Å, and that of fcc Au is chosen as $a_{\mathrm{Au}} = \sqrt{2}a_{\mathrm{Fe}} = 4.054$ Å. For Cu(111)|Co(0001) we use the experimental lattice constant $a_{\mathrm{Co}} = 2.507$ Å, and a c/a ratio of 1.623. For Cu|Ni(111) $a_{\mathrm{Ni}} = 3.524$ Å is used. In both cases, the fcc Cu leads are slightly stretched to match.
[24] The areas of the primitive 2D BZs for Co and Ni are almost identical and more than twice as large as that for Fe. Therefore the **k**-point sampling densities in the transport calculations for all three systems are very similar.
[25] K. M. Schep, J. B. A. N. van Hoof, P. J. Kelly, G. E. W. Bauer, and J. E. Inglesfield, Phys. Rev. B **56**, 10805 (1997).
[26] S. Y. Savrasov and D. Y. Savrasov, Phys. Rev. B **54**, 16487 (1996).
[27] *CRC Handbook of Chemistry and Physics*, 84th ed., edited by D. R. Lide (CRC Press, Boca Raton, FL, 2003).
[28] Resistivity-like and conductivity-like regimes are determined by whether additional disorder increases or decreases the damping.
[29] *American Institute of Physics Handbook*, 3rd ed., edited by D. E. Gray (McGraw-Hill, New York, 1972).
[30] J. D. Jackson, *Classical Electrodynamics*, 3rd ed. (Wiley, New York, 1999).
[31] A. S. Arrott, in *Ultrathin Magnetic Structures I*, edited by J. A. C. Bland and B. Heinrich (Springer, New York, 1994), pp. 7–19.
[32] C. Scheck, L. Cheng, I. Barsukov, Z. Frait, and W. E. Bailey, Phys. Rev. Lett. **98**, 117601 (2007).

Unified First-Principles Study of Gilbert Damping, Spin-Flip Diffusion, and Resistivity in Transition Metal Alloys

Anton A. Starikov,[1] Paul J. Kelly,[1] Arne Brataas,[2] Yaroslav Tserkovnyak,[3] and Gerrit E. W. Bauer[4]

[1]*Faculty of Science and Technology and* MESA$^+$ *Institute for Nanotechnology, University of Twente, P.O. Box 217, 7500 AE Enschede, The Netherlands*

[2]*Department of Physics, Norwegian University of Science and Technology, N-7491 Trondheim, Norway*

[3]*Department of Physics and Astronomy, University of California, Los Angeles, California 90095, USA*

[4]*Kavli Institute of NanoScience, Delft University of Technology, Lorentzweg 1, 2628 CJ Delft, The Netherlands*

(Received 23 July 2010; published 2 December 2010)

Using a formulation of first-principles scattering theory that includes disorder and spin-orbit coupling on an equal footing, we calculate the resistivity ρ, spin-flip diffusion length l_{sf}, and Gilbert damping parameter α for $Ni_{1-x}Fe_x$ substitutional alloys as a function of x. For the technologically important $Ni_{80}Fe_{20}$ alloy, Permalloy, we calculate values of $\rho = 3.5 \pm 0.15\ \mu\Omega\,\mathrm{cm}$, $l_{\mathrm{sf}} = 5.5 \pm 0.3$ nm, and $\alpha = 0.0046 \pm 0.0001$ compared to experimental low-temperature values in the range 4.2–4.8 $\mu\Omega\,\mathrm{cm}$ for ρ, 5.0–6.0 nm for l_{sf}, and 0.004–0.013 for α, indicating that the theoretical formalism captures the most important contributions to these parameters.

DOI: 10.1103/PhysRevLett.105.236601 PACS numbers: 72.25.Rb, 71.70.Ej, 72.25.Ba, 75.40.Gb

Introduction.—The drive to increase the density and speed of magnetic forms of data storage has focused attention on how magnetization changes in response to external fields and currents, on shorter length and time scales [1]. The dynamics of a magnetization $\mathbf{M}$ in an effective magnetic field $\mathbf{H}_{\mathrm{eff}}$ is commonly described using the phenomenological Landau-Lifshitz-Gilbert equation

$$\frac{d\mathbf{M}}{dt} = -\gamma \mathbf{M} \times \mathbf{H}_{\mathrm{eff}} + \mathbf{M} \times \left[\frac{\tilde{G}(\mathbf{M})}{\gamma M_s^2} \frac{d\mathbf{M}}{dt} \right], \qquad (1)$$

where $M_s = |\mathbf{M}|$ is the saturation magnetization, $\tilde{G}(\mathbf{M})$ is the Gilbert damping parameter (that is, in general, a tensor), and the gyromagnetic ratio $\gamma = g\mu_B/\hbar$ is expressed in terms of the Bohr magneton μ_B and the Landé g factor, which is approximately 2 for itinerant ferromagnets. The *time* decay of a magnetization precession is frequently expressed in terms of the dimensionless parameter α given by the diagonal element of $\tilde{G}/\gamma M_s$ for an isotropic medium. If a nonequilibrium magnetization is generated in a disordered metal (for example, by injecting a current through an interface), its *spatial* decay is described by the diffusion equation

$$\frac{\partial^2 \Delta\mu}{\partial z^2} = \frac{\Delta\mu}{l_{\mathrm{sf}}^2} \qquad (2)$$

in terms of the spin accumulation $\Delta\mu$, the difference between the spin-dependent electrochemical potentials μ^σ for up and down spins, and the spin-flip diffusion length l_{sf} [2,3]. In spite of the great importance of α and l_{sf}, our understanding of the factors that contribute to their numerical values is, at best, sketchy. For clean ferromagnetic metals [4] and ordered alloys [5] however, recent progress has been made in calculating the Gilbert damping using the torque correlation model [6] and the relaxation time approximation in the framework of the Boltzmann equation. Estimating the relaxation time for particular materials and scattering mechanisms is, in general, a nontrivial task, and application of the torque correlation model to nonperiodic systems entails many additional complications and has not yet been demonstrated. Thus, the theoretical study of Gilbert damping or spin-flip scattering in disordered alloys and their calculation for particular materials with intrinsic disorder remain open questions.

Method.—In this Letter we calculate the resistivity ρ, spin-flip diffusion length l_{sf}, and Gilbert damping parameter α for substitutional $Ni_{1-x}Fe_x$ alloys within a single first-principles framework. To do so, we have extended a scattering formalism [7] based upon the local spin density approximation of density functional theory so that spin-orbit coupling (SOC) and chemical disorder are included on an equal footing. Relativistic effects are included by using the Pauli Hamiltonian.

For a disordered region of ferromagnetic (FM) alloy sandwiched between leads of nonmagnetic (NM) material, the scattering matrix S relates incoming and outgoing states in terms of reflection (r) and transmission (t) matrices at the Fermi energy. To calculate the scattering matrix, we use a ''wave-function matching'' scheme [7] implemented with a minimal basis of tight-binding linearized muffin-tin orbitals [8]. Atomic-sphere-approximation potentials [8] are calculated self-consistently using a surface Green's function method, also implemented [9] with tight-binding linearized muffin-tin orbitals. Charge and spin densities for binary alloy A and B sites are calculated using the coherent potential approximation (CPA) [10]

generalized to layer structures [9]. For the transmission matrix calculation, the resulting spherical potentials are assigned randomly to sites in large lateral supercells subject to maintenance of the appropriate concentration of the alloy [7]. Solving the transport problem using lateral supercells makes it possible to go beyond effective medium approximations such as the CPA. Because we are interested in the properties of bulk alloys, the leads can be chosen for convenience, and we use Cu leads with a single scattering state for each value of crystal momentum, $\mathbf{k}_\parallel$. The alloy lattice constants are determined using Vegard's law, and the lattice constants of the leads are made to match. Though NiFe is fcc only for the concentration range $0 \leq x \leq 0.6$, we use the fcc structure for all values of x.

For the self-consistent surface Green's function calculations (without SOC), the two-dimensional (2D) Brillouin zone (BZ) corresponding to the 1×1 interface unit cell was sampled with a 120×120 grid. Transport calculations including spin-orbit coupling were performed with a 32×32 2D BZ grid for a 5×5 lateral supercell, which is equivalent to a 160×160 grid in the 1×1 2D BZ. The thickness of the ferromagnetic layer ranged from 3 to 200 monolayers of fcc alloy; for the largest thicknesses, the scattering region contained more than 5000 atoms. For every thickness of ferromagnetic alloy, we averaged over a number of random disorder configurations; the sample to sample spread was small, and typically only five configurations were necessary.

Resistivity.—We calculate the electrical resistivity to illustrate our methodology. In the Landauer-Büttiker formalism, the conductance can be expressed in terms of the transmission matrix t as $G = (e^2/h)\mathrm{Tr}\{tt^\dagger\}$ [11,12]. The resistance of the complete system consisting of ideal leads sandwiching a layer of ferromagnetic alloy of thickness L is $R(L) = 1/G(L) = 1/G_{\mathrm{Sh}} + 2R_{\mathrm{if}} + R_b(L)$, where $G_{\mathrm{Sh}} = (2e^2/h)N$ is the Sharvin conductance of each lead with N conductance channels per spin, R_{if} is the interface resistance of a single NM|FM interface, and $R_b(L)$ is the bulk resistance of a ferromagnetic layer of thickness L [7,13]. When the ferromagnetic slab is sufficiently thick, Ohmic behavior is recovered whereby $R_b(L) \approx \rho L$, as shown in the inset to Fig. 1 for Permalloy ($\mathrm{Py} = \mathrm{Ni_{80}Fe_{20}}$), and the bulk resistivity ρ can be extracted from the slope of $R(L)$ [14]. For currents parallel and perpendicular to the magnetization direction, the resistivities are different and have to be calculated separately. The average resistivity is given by $\bar{\rho} = (\rho_\parallel + 2\rho_\perp)/3$, and the anisotropic magnetoresistance ratio (AMR) is $(\rho_\parallel - \rho_\perp)/\bar{\rho}$.

For Permalloy we find values of $\bar{\rho} = 3.5 \pm 0.15\ \mu\Omega\,\mathrm{cm}$ and $\mathrm{AMR} = 19 \pm 1\%$, compared to experimental low-temperature values in the range 4.2–4.8 $\mu\Omega\,\mathrm{cm}$ for $\bar{\rho}$ and 18% for AMR [15]. The resistivity calculated as a function of x is compared to low-temperature values from the literature [15] in Fig. 1. The plateau in the calculated values around the Py composition appears to be seen in the

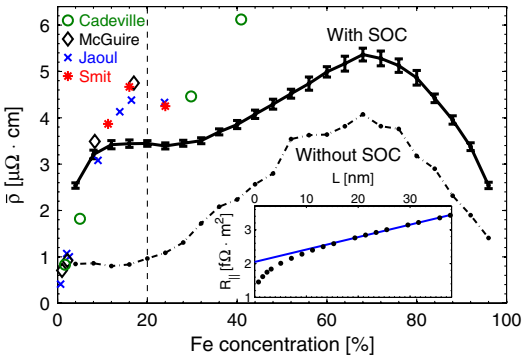

FIG. 1 (color online). Calculated resistivity as a function of the concentration x for fcc $\mathrm{Ni}_{1-x}\mathrm{Fe}_x$ binary alloys with (solid line) and without (dashed-dotted line) SOC. Low-temperature experimental results are shown as symbols [15]. The composition $\mathrm{Ni_{80}Fe_{20}}$ is indicated by a vertical dashed line. Inset: resistance of $\mathrm{Cu|Ni_{80}Fe_{20}|Cu}$ as a function of the thickness of the alloy layer. Dots indicate the calculated values averaged over five configurations, while the solid line is a linear fit.

experiments by Smit and Jaoul *et al.* [15]. The overall agreement with previous calculations is good [16]. In spite of the smallness of the SOC, the resistivity of Py is underestimated by more than a factor of 4 when it is omitted, underlining its importance for understanding transport properties.

Three sources of disorder which have not been taken into account here will increase the calculated values of ρ: short range potential fluctuations that go beyond the single site CPA, short range strain fluctuations reflecting the differing volumes of Fe and Ni, and spin disorder. These will be the subject of a later study.

Gilbert damping.—Recently, Brataas *et al.* showed that the energy loss due to Gilbert damping in an NM|FM|NM scattering configuration can be expressed in terms of the scattering matrix S [17]. Using the Landau-Lifshitz-Gilbert equation (1), the energy lost by the ferromagnetic slab is

$$\frac{dE}{dt} = \frac{d}{dt}(\mathbf{H}_{\mathrm{eff}} \cdot \mathbf{M}) = \mathbf{H}_{\mathrm{eff}} \cdot \frac{d\mathbf{M}}{dt} = \frac{1}{\gamma^2}\frac{d\mathbf{m}}{dt}\tilde{G}(\mathbf{M})\frac{d\mathbf{m}}{dt}, \tag{3}$$

where $\mathbf{m} = \mathbf{M}/M_s$ is the unit vector of the magnetization direction for the macrospin mode. By equating this energy loss to the energy flow into the leads [18] associated with "spin pumping" [19],

$$I_E^{\mathrm{Pump}} = \frac{\hbar}{4\pi}\mathrm{Tr}\left\{\frac{dS}{dt}\frac{dS^\dagger}{dt}\right\} = \frac{\hbar}{4\pi}\mathrm{Tr}\left\{\frac{dS}{d\mathbf{m}}\frac{d\mathbf{m}}{dt}\frac{dS^\dagger}{d\mathbf{m}}\frac{d\mathbf{m}}{dt}\right\}, \tag{4}$$

the elements of the tensor $\tilde{G}$ can be expressed as

$$\tilde{G}_{i,j}(\mathbf{m}) = \frac{\gamma^2\hbar}{4\pi}\mathrm{Re}\left\{\mathrm{Tr}\left[\frac{\partial S}{\partial m_i}\frac{\partial S^\dagger}{\partial m_j}\right]\right\}. \tag{5}$$

Physically, energy is transferred slowly from the spin degrees of freedom to the electronic orbital degrees of

freedom, from where it is rapidly lost to the phonon degrees of freedom. Our calculations focus on the role of elastic scattering in the rate-limiting first step.

Assuming that the Gilbert damping is isotropic for cubic substitutional alloys and allowing for the enhancement of the damping due to the FM|NM interfaces [19–21], the total damping in the system with a ferromagnetic slab of thickness L can be written $\tilde{G}(L) = \tilde{G}_{\rm if} + \tilde{G}_b(L)$, where we express the bulk damping in terms of the dimensionless Gilbert damping parameter $\tilde{G}_b(L) = \alpha\gamma M_s(L) = \alpha\gamma\tilde{\mu}_s AL$, where $\tilde{\mu}_s$ is the magnetization density and A is the cross section. The results of calculations for $Ni_{80}Fe_{20}$ are shown in the inset to Fig. 2, where the derivatives of the scattering matrix in (5) were evaluated numerically by taking finite differences. The intercept at $L = 0$, $\tilde{G}_{\rm if}$, allows us to extract the damping enhancement [20], but here we focus on the bulk properties and leave consideration of the material dependence of the interface enhancement for later study. The value of α determined from the slope of $\tilde{G}(L)/(\gamma\tilde{\mu}_s A)$ is 0.0046 ± 0.0001, which is at the lower end of the range of values 0.004–0.013 measured at room temperature for Py [21–23].

Figure 2 shows the Gilbert damping parameter as a function of x for $Ni_{1-x}Fe_x$ binary alloys in the fcc structure. From a large value for clean Ni, it decreases rapidly to a minimum at $x \sim 0.65$ and then grows again as the limit of clean fcc Fe is approached. Part of the decrease in α with increasing x can be explained by the increase in the magnetic moment per atom as we progress from Ni to Fe. The large values of α calculated in the dilute alloy limits can be understood in terms of conductivity-like enhancement at low temperatures [24], which has been explained in terms of intraband scattering [4,6]. The trend exhibited by the theoretical $\alpha(x)$ is seen to be reflected by experimental room-temperature results. In spite of a large spread in measured values, these seem to be systematically larger

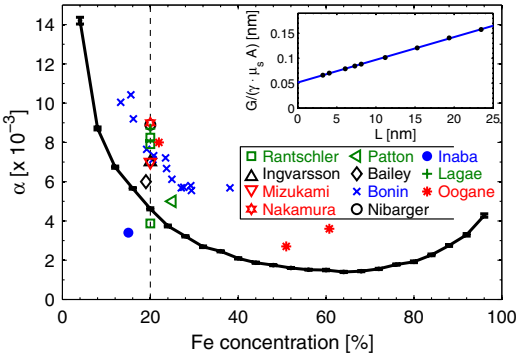

FIG. 2 (color online). Calculated zero-temperature (solid line) and experimental room-temperature (symbols) values of the Gilbert damping parameter as a function of the concentration x for fcc $Ni_{1-x}Fe_x$ binary alloys [21–23]. Inset: total damping of $Cu|Ni_{80}Fe_{20}|Cu$ as a function of the thickness of the alloy layer. Dots indicate the calculated values averaged over five configurations, while the solid line is a linear fit.

than the calculated values. Part of this discrepancy can be attributed to an increase in α with temperature [22,25].

Spin diffusion.—When an unpolarized current is injected from a normal metal into a ferromagnet, the polarization will return to the value characteristic of the bulk ferromagnet sufficiently far from the injection point, provided there are processes which allow spins to flip. Following Valet and Fert [3] and assuming there is no spin-flip scattering in the NM leads, we can express the fractional spin-current densities $p^{\uparrow(\downarrow)} = J^{\uparrow(\downarrow)}/J$ as a function of distance z from the interface as

$$p^{\uparrow(\downarrow)}(z) = \frac{1}{2} \pm \frac{\beta}{2}\left[1 - \frac{\exp(-z/l_{\rm sf})r^*_{\rm if}(\beta - \gamma + \gamma\delta)}{\beta(r^*_{\rm if} + l_{\rm sf}\delta\rho^*_{\rm F}\tanh\delta)}\right], \tag{6}$$

where J is the total current through the device, $J^\uparrow$ and $J^\downarrow$ are the currents of majority and minority electrons, respectively, $l_{\rm sf}$ is the spin-diffusion length, $\rho^*_F = (\rho^\downarrow + \rho^\uparrow)/4$ is the bulk resistivity, and β is the bulk spin asymmetry $(\rho^\downarrow - \rho^\uparrow)/(\rho^\downarrow + \rho^\uparrow)$. The interface resistance $r^*_{\rm if} = (r^\downarrow_{\rm if} + r^\uparrow_{\rm if})/4$, the interface resistance asymmetry $\gamma = (r^\downarrow_{\rm if} - r^\uparrow_{\rm if})/(r^\downarrow_{\rm if} + r^\uparrow_{\rm if})$, and the interface spin-relaxation expressed through the spin-flip coefficient δ [26] must be taken into consideration, resulting in a finite polarization of the current injected into the ferromagnet. The corresponding expressions are plotted as solid lines in Fig. 3.

To calculate the spin-diffusion length we inject nonpolarized states from one NM lead and probe the transmission probability into different spin channels in the other NM lead for different thicknesses of the ferromagnet. Figure 3 shows that the calculated values can be fitted using expressions (6) if we assume that $J^\sigma/J = G^\sigma/G$, yielding values of the spin-flip diffusion length $l_{\rm sf} = 5.5 \pm 0.3$ nm and bulk asymmetry parameter $\beta = 0.678 \pm 0.003$ for $Ni_{80}Fe_{20}$ alloy, compared to experimentally estimated values of 0.7 ± 0.1 for β and in the range 5.0–6.0 nm for $l_{\rm sf}$ [27].

$l_{\rm sf}$ and β are shown as a function of the concentration x in Fig. 4. The convex behavior of β is dominated by and

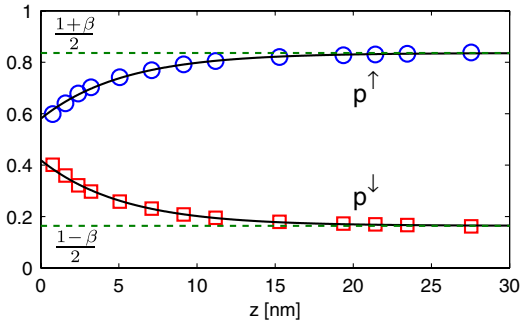

FIG. 3 (color online). Fractional spin-current densities for electrons injected at $z = 0$ from Cu into $Ni_{80}Fe_{20}$ alloy. Symbols indicate calculated values, while the solid lines are fits to Eq. (6).

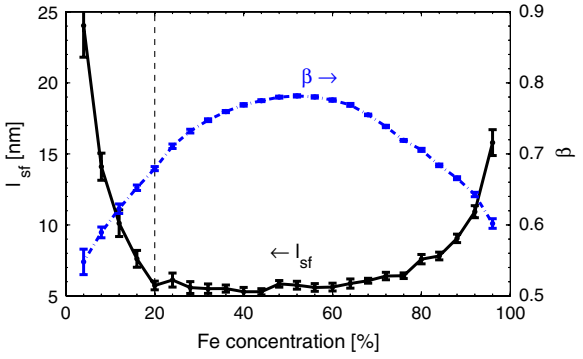

FIG. 4 (color online). Spin-diffusion length (solid line) and polarization β as a function of the concentration x for $Ni_{1-x}Fe_x$ binary alloys.

tracks the large minority spin resistivity $\rho^{\downarrow}$ whose origin is the large mismatch of the Ni and Fe minority spin band structures that leads to a $\sim x(1-x)$ concentration dependence of $\rho^{\downarrow}(x)$ [16]. The majority spin band structures match well, so $\rho^{\uparrow}$ is much smaller and changes relatively weakly as a function of x. The increase of l_{sf} in the clean metal limits corresponds to the increase of the electron momentum and spin-flip scattering times in the limit of weak disorder.

In summary, we have developed a unified density functional theory-based scattering theoretical approach for calculating transport parameters of concentrated alloys that depend strongly on spin-orbit coupling and disorder and have illustrated it with an application to NiFe alloys. Where comparison with experiment can be made, the agreement is remarkably good, offering the prospect of gaining insight into the properties of a host of complex but technologically important magnetic materials.

This work is part of the research program of the "Stichting voor Fundamenteel Onderzoek der Materie," and the use of supercomputer facilities was sponsored by the "Stichting Nationale Computer Faciliteiten," both financially supported by the "Nederlandse Organisatie voor Wetenschappelijk Onderzoek." This work was also supported by "NanoNed," a nanotechnology programme of the Dutch Ministry of Economic Affairs, by EC Contract No. IST-033749 DynaMax, and by EU FP7 ICT Grant No. 251759 MACALO.

[1] See the collection of articles in *Ultrathin Magnetic Structures I–IV*, edited by J. A. C. Bland and B. Heinrich (Springer-Verlag, Berlin, 1994).
[2] P. C. van Son, H. van Kempen, and P. Wyder, Phys. Rev. Lett. **58**, 2271 (1987); **60**, 378 (1988).
[3] T. Valet and A. Fert, Phys. Rev. B **48**, 7099 (1993).
[4] K. Gilmore, Y. U. Idzerda, and M. D. Stiles, Phys. Rev. Lett. **99**, 027204 (2007); J. Appl. Phys. **103**, 07D303 (2008); V. Kamberský, Phys. Rev. B **76**, 134416 (2007).
[5] C. Liu *et al.*, Appl. Phys. Lett. **95**, 022509 (2009).
[6] V. Kamberský, Czech. J. Phys. **26**, 1366 (1976).
[7] K. Xia *et al.*, Phys. Rev. B **63**, 064407 (2001); **73**, 064420 (2006).
[8] O. K. Andersen, Z. Pawlowska, and O. Jepsen, Phys. Rev. B **34**, 5253 (1986); O. K. Andersen, *ibid.* **12**, 3060 (1975).
[9] I. Turek *et al.*, *Electronic Structure of Disordered Alloys, Surfaces and Interfaces* (Kluwer, Boston-London-Dordrecht, 1997).
[10] P. Soven, Phys. Rev. **156**, 809 (1967).
[11] M. Büttiker *et al.*, Phys. Rev. B **31**, 6207 (1985).
[12] S. Datta, *Electronic Transport in Mesoscopic Systems* (Cambridge University Press, Cambridge, England, 1995).
[13] K. M. Schep *et al.*, Phys. Rev. B **56**, 10805 (1997).
[14] The nonlinearity of the resistance for $L \lesssim 20$ in the inset to Fig. 1 has nothing to do with spin-orbit coupling. It results when spin-dependent resistances of the form $R^{\sigma}(L) = 2/G_{Sh} + 2R^{\sigma}_{if} + \rho^{\sigma}L$ are added in parallel in the two-current series-resistor model; the total resistance only becomes linear for values of L so large that the bulk resistances $\rho^{\sigma}L$ are much larger than the interface and Sharvin terms.
[15] J. Smit, Physica (Amsterdam) **17**, 612 (1951); T. R. McGuire and R. I. Potter, IEEE Trans. Magn. **11**, 1018 (1975); O. Jaoul, I. A. Campbell, and A. Fert, J. Magn. Magn. Mater. **5**, 23 (1977); M. C. Cadeville and B. Loegel, J. Phys. F **3**, L115 (1973).
[16] J. Banhart and H. Ebert, Europhys. Lett. **32**, 517 (1995); J. Banhart, H. Ebert, and A. Vernes, Phys. Rev. B **56**, 10165 (1997).
[17] A. Brataas, Y. Tserkovnyak, and G. E. W. Bauer, Phys. Rev. Lett. **101**, 037207 (2008).
[18] J. E. Avron *et al.*, Phys. Rev. Lett. **87**, 236601 (2001); M. Moskalets and M. Büttiker, Phys. Rev. B **66**, 035306 (2002); **66**, 205320 (2002).
[19] Y. Tserkovnyak, A. Brataas, and G. E. W. Bauer, Phys. Rev. Lett. **88**, 117601 (2002); Phys. Rev. B **66**, 224403 (2002).
[20] M. Zwierzycki *et al.*, Phys. Rev. B **71**, 064420 (2005).
[21] S. Mizukami, Y. Ando, and T. Miyazaki, J. Magn. Magn. Mater. **226–230**, 1640 (2001); Jpn. J. Appl. Phys. **40**, 580 (2001).
[22] W. Bailey *et al.*, IEEE Trans. Magn. **37**, 1749 (2001).
[23] C. E. Patton, Z. Frait, and C. H. Wilts, J. Appl. Phys. **46**, 5002 (1975); S. Ingvarsson *et al.*, Appl. Phys. Lett. **85**, 4995 (2004); H. Nakamura *et al.*, Jpn. J. Appl. Phys. **43**, L787 (2004); J. O. Rantschler *et al.*, IEEE Trans. Magn. **41**, 3523 (2005); R. Bonin *et al.*, J. Appl. Phys. **98**, 123904 (2005); L. Lagae *et al.*, J. Magn. Magn. Mater. **286**, 291 (2005); J. P. Nibarger *et al.*, Appl. Phys. Lett. **83**, 93 (2003); N. Inaba *et al.*, IEEE Trans. Magn. **42**, 2372 (2006); M. Oogane *et al.*, Jpn. J. Appl. Phys. **45**, 3889 (2006).
[24] S. M. Bhagat and P. Lubitz, Phys. Rev. B **10**, 179 (1974); B. Heinrich, D. J. Meredith, and J. F. Cochran, J. Appl. Phys. **50**, 7726 (1979).
[25] D. Bastian and E. Biller, Phys. Status Solidi A **35**, 113 (1976).
[26] W. Park *et al.*, Phys. Rev. B **62**, 1178 (2000).
[27] J. Bass and W. P. Pratt, Jr., J. Magn. Magn. Mater. **200**, 274 (1999); J. Phys. Condens. Matter **19**, 183201 (2007).